Soil & Tillage Research 262 (2026) 107234

Contents lists available at ScienceDirect

Soil & Tillage Research

journal homepage: www.elsevier.com/locate/still

Biochar dominated the combined effect of silicate rock powder and biochar application on extracellular enzyme kinetics and nutrient dynamics in a sandy soil

Maria Ansari[a,*], Svenja Stock[b], Michaela A. Dippold[b], Susanne E. Hamburger[c], Claudia I. Kammann[c], Johannes Meyer zu Drewer[d,e,f], Nikolas Hagemann[d,e], Annette Eschenbach[a], Joscha N. Becker[a]

[a] Institute of Soil Science, University of Hamburg, Hamburg, Germany
[b] Geo-Biosphere Interactions, Department of Geosciences, Eberhard Karls University of Tübingen, Tübingen, Germany
[c] Department of Applied Ecology, Hochschule Geisenheim University, Geisenheim, Germany
[d] Ithaka Institute, Goldbach, Germany
[e] Agroscope, Zurich, Switzerland
[f] Institute for Sustainable Energy Systems, Offenburg University, Offenburg, Germany

ARTICLE INFO

Keywords:
Basanite
Carbon dioxide removal (CDR)
Nutrient demand
Rock-enhanced biochar
Enhanced rock weathering (ERW)
Fluorometric enzyme assay

ABSTRACT

The application of biochar or silicate rock powder as soil amendments combines carbon dioxide removal with soil improvement. However, their combined short-term effects on nutrient dynamics and microbial activity are poorly understood. Therefore, we combined wood biochar and basanite powder via co-application and via co-pyrolysis of biomass and basanite to rock-enhanced biochar in a nine-week semi-field-based lysimeter experiment with cabbage turnip (*Brassica oleracea* var. *gongylodes* L.). We measured carbon (C), nitrogen (N), available phosphorous (P), mineral N, dissolved organic C (DOC), microbial biomass C (C_{mic}), soil pH, and electric conductivity (EC). We examined extracellular enzyme kinetics of ß-glucosidase (BG), chitinase (CH), leucine-aminopeptidase (LAP), and acid phosphatase (AP) related to C, N, and P cycles. From potential enzyme activity (V_{max}) of BG, LAP, and AP we calculated extracellular enzyme stoichiometry (EES), vector angle and length to assess nutrient limitations.

In combined applications, the influence of biochar was dominant. The application of biochar-containing amendments (biochar, co-application, co-pyrolyzed rock-enhanced biochar) to our sandy topsoil significantly increased C, P, DOC, C_{mic}, pH, and EC. Co-application even exceeded single biochar in increasing N, pH, and EC. Single biochar application resulted in the highest short-term P availability, while combined applications potentially result in a long-term P supply. While LAP's V_{max} increased following biochar-containing amendment application, V_{max} of the other enzymes decreased. Although AP showed the highest V_{max}, indicating a P limitation, the enzyme patterns and EES suggest an increased N demand and a shift from P-limited towards a more balanced microbial nutrient demand following biochar-containing amendment application.

1. Introduction

Biochar is a carbon-rich solid produced from biomass by pyrolysis (Hagemann et al., 2018; Lehmann and Joseph, 2024) and is traditionally used as a soil amendment around the world (Allen, 1847; Glaser et al., 2001; Wiedner et al., 2015). Due to its high aromaticity, biochar carbon is barely bioavailable and largely stabilized against decomposition (Zimmerman, 2010; Ameloot et al., 2013; Kuzyakov et al., 2014; Wang et al., 2016). Thus, soil-applied biochars are a long-term carbon (C) sink (Steiner et al., 2007; Rechberger et al., 2017; Lehmann et al., 2021) providing carbon dioxide removal (CDR). Nevertheless, biochars contain a labile fraction consisting of more easily available C and nutrients (Bakshi et al., 2018; Zhao et al., 2018). Biochars can maintain or improve soil properties (Joseph et al., 2010; Schmidt et al., 2021), e.g. by increasing soil pH (Chintala et al., 2014; Dai et al., 2017) and enhancing nutrient availability (Glaser and Lehr, 2019; Hossain et al.,

* Corresponding author.
E-mail address: maria.ansari@uni-hamburg.de (M. Ansari).

https://doi.org/10.1016/j.still.2026.107234
Received 15 October 2025; Received in revised form 18 March 2026; Accepted 19 April 2026
Available online 22 April 2026

2020; Bekchanova et al., 2024). The application of biochars often result in an increased microbial biomass C (C_{mic}) as well as microbial activity and can shift microbial community composition, which in turn may alter nutrient cycles and affect plant growth (Lehmann et al., 2011; Buss et al., 2021).

Silicate rock powder is applied to agricultural soils for enhanced rock weathering (ERW) as a CDR technology and due to its potential to influence key soil properties and thus increase soil fertility (Abdalqadir et al., 2024; Dupla et al., 2024) and yield (Haque et al., 2020; Swoboda et al., 2022). During silicate rock weathering, cations and anions, such as potassium and phosphorus (P), are released (Amann et al., 2020; Guo et al., 2023; Beerling et al., 2025), resulting in an increased nutrient content (Buss et al., 2023). Silicate rock powder application can increase soil pH (Swoboda et al., 2022; Xu et al., 2024a) and by this increase the availability of nutrients, such as P, even further (Swoboda et al., 2022; Beerling et al., 2025). These changes in soil properties can result in an altered C_{mic} (Sokol et al., 2024; Xu et al., 2024b) and a shift in microbial community (Carson et al., 2007; Zhou et al., 2018). The activity of soil microorganisms can in return stimulate the weathering of silicate rock powder (Buss et al., 2021; Li et al., 2025; Reginato, 2025). Even though Vicca et al. (2022) underlined the importance of biological processes for the efficiency of ERW, little is known about the coupling between ERW and soil microorganisms.

Most recent research considered biochar and silicate rock powder separately, while their combined application could offer synergistic effects for CDR as well as for key soil properties and processes, such as nutrient cycles and microbial activity (Amann and Hartmann, 2019; Buss et al., 2021). In addition to simple co-application, co-pyrolysis of biomass and rock powder to rock-enhanced biochar provides another potential approach to combine those soil amendments (Meyer zu Drewer et al., 2025; Vorrath et al., 2025). The effects of such combined applications of those two amendments on soil properties, including nutrient dynamics and microbial processes, is currently unknown.

Soil microorganisms produce and release extracellular enzymes to meet their nutrient demand (Allison et al., 2011; Jin et al., 2024). These extracellular enzymes can trigger the degradation of complex organic substances into smaller molecules (Shi, 2011), thereby enhancing nutrient availability for microbial uptake (Allison et al., 2011; Jin et al., 2024). However, after their release, extracellular enzymes can be adsorbed to reactive particle surfaces, such as soil organic matter (Allison, 2006; Burns et al., 2013; Luo et al., 2017) or biochar (Lehmann et al., 2011). Despite this immobilization, absorbed enzymes remain a significant reservoir of potential enzyme activity, responding rapidly to changes in nutrient availability (Burns et al., 2013). Consequently, extracellular enzymes serve as valuable indicators for nutrient cycling and availability in soils (Luo et al., 2017). The enzyme ß-glucosidase (BG) is one of the primary catalysts of cellulose degradation to glucose and thus plays an important role in the soil C cycle (Bakshi and Varma, 2011; Moorhead et al., 2016). Chitinase (CH) is responsible for the degradation of chitin and is part of both C and nitrogen (N) cycle in soils (Bakshi and Varma, 2011). Leucine-aminopeptidase (LAP) can catalyze the cleavage of leucine amino acid from peptide substrates, such as proteins, and thus is an indicative part of the soil N cycle (Moorhead et al., 2016). Acid phosphatase (AP) can catalyze the hydrolysis of esters and anhydrides of phosphoric acids, leading to a release of inorganic P for soil microbes and plants (Bakshi and Varma, 2011; Moorhead et al., 2016). The ratios of the potential activities of these enzymes involved in C, N, and P cycling, referred to as extracellular enzyme stoichiometry (EES), and the resulting enzymatic C:N:P ratio can indicate microbial nutrient limitations (Sinsabaugh et al., 2008; Yang et al., 2020).

It has not been studied yet how the combined application of biochar and silicate rock powder, such as basanite, to soils influence nutrient cycles and microbial enzyme kinetics. We hypothesize that the combined application of biochar and basanite (i) significantly improves soil properties relevant to microbial activity, leading to changes in (ii) the extracellular enzyme kinetics of BG, CH, AP, and LAP as well as (iii) EES, compared to unamended soils. We further investigate how these effects compare to those of single biochar or single basanite application. The combined application of biochar and basanite was tested as a simple co-application of both amendments and as rock-enhanced biochar. We conducted a semi-field experiment in lysimeters using sandy agricultural soil (control) amended with either biochar (biochar treatment), basanite powder (rock powder treatment), rock-enhanced biochar (co-pyrolysis treatment), or the co-application of biochar and basanite powder (co-application treatment). We sampled and analyzed the soil samples after the plant harvest for soil properties, such as pH and exchangeable nutrients, and conducted a fluorometric enzyme assay followed by EES calculations.

2. Materials and Methods

2.1. Soils and amendments

The study was conducted using a sandy arable topsoil (0–30 cm; Table 1). The soil was collected in summer 2023 in Northern Germany (Gräflich Bernstorff'sche Betriebe, Gartow, Germany, 53°01'26.9"N 11°27'12.7"E) and was air-dried until used in summer 2024.

We used four different soil amendments for this study. The biochar was produced from a mixture of wood chips and woody sieving residues from green waste composting in a weight-ratio of 1:1. This woody biomass was pyrolyzed at 650 °C for 20 min on a Pyreg 500 (Pyreg GmbH, Dörth, Germany) full scale commercial pyrolysis unit (Sonnenerde GmbH, Riedlingsdorf, Austria) (Table 1). As silicate rock powder, we used the locally available basanite *Eifelgold* with a grain size between 0.5 and 300 µm (further information in Table A.1). Additionally, two combined applications of biochar and basanite were used – co-application and co-pyrolysis. For the latter, the woody biomass and basanite were mixed in a weight-ratio of 80:20, pelletized, and afterwards pyrolyzed at 650 °C for 20 min to produce rock-enhanced biochar (Table 1). Based on the TOC contents of biochar and rock-enhanced biochar, we calculated that the rock-enhanced biochar consisted of ~68% biochar and ~32% basanite. To compare the effect of combined pyrolysis to a simple mixing, we co-applied biochar and basanite in the same ratio as found in the rock-enhanced biochar. More detailed information about the amendments can be found in Meyer zu Drewer et al. (2025).

Table 1
Properties of temperate sandy agricultural topsoil, biochar, and rock-enhanced biochar.

Properties	Soil[a]	Biochar[b]	Rock-enhanced-biochar[b]
pH [$CaCl_2$]	4.7 ± 0.0	9.0	9.2
CEC [$mmol_c\ kg^{-1}$]	21.3 ± 0.6	n.d.	n.d.
C [$g\ kg^{-1}$]	12.4 ± 0.0	494	336
TOC [$g\ kg^{-1}$]	12.0 ± 0.0	482	332
TIC [$g\ kg^{-1}$]	0.4 ± 0.0	12	4
N [$g\ kg^{-1}$]	1.1 ± 0.0	7.0	4.1
C:N	11.6 ± 0.0	80	82
H:C	n.d.	0.35	0.23
O:C	n.d.	0.14	0.08
P_2O_5 [$g\ kg^{-1}$]	n.d.	9	8
Ash [%]	n.d.	44.3	62.9
Sand [%]	93.83 ± 1.15	n.a.	n.a.
Silt [%]	2.47 ± 0.77	n.a.	n.a.
Clay [%]	3.70 ± 0.46	n.a.	n.a.

[a] Values are the mean of analytical replicates (n = 3, mean ± standard deviation), [b] values were measured by Eurofins according to the analytical guidelines of the European Biochar Certificate (EBC, 2024). CEC = cation exchange capacity, C = total carbon, TOC = total organic carbon, TIC = total inorganic carbon, N = total nitrogen, n.d. = not determined, n.a. = not applicable.

2.2. Experimental design

We used 45 lysimeters (each 20 cm diameter, 30 cm soil depth, stainless steel mesh allowing drainage into a catchment vessel below) consisting of five treatments (n = 9). The lysimeter tubes with their catchment vessels were embedded in sand beds to enable closer-to-natural soil temperatures compared to pot experiments. The leachate in the catchment vessel was pumped out regularly to prevent water accumulation. Inside the lysimeters, bags consisting of PVC were installed to contain the samples. For the control treatment, the bags inside the lysimeters were filled with 9 kg of soil (dry weight equivalent). For the biochar treatment, 379.1 g of biochar (equals ~4.2 wt%) was mixed with the soil and the mixture was filled into the respective bags and installed in the lysimeters. The rock powder treatment contained soil mixed with 178.2 g of basanite powder (equals ~2 wt%). The co-pyrolysis treatment was filled with a mixture of soil and 557.3 g of rock-enhanced biochar (equals ~6.2 wt% consisting of ~4.2 wt% biochar and ~2 wt% basanite powder). For the equivalent co-application treatment, the bag within the lysimeter was filled with a mixture of soil, 379.1 g of biochar (equals ~4.2 wt%), and 178.2 g of basanite powder (equals ~2 wt%). The lysimeters containing the different treatments were arranged in a randomized complete block design (Fig. A.1). Every lysimeter was planted with one cabbage turnip (*Brassica oleracea* var. *gongylodes* L.) seedling each. The seedlings were as similar as possible in development and strength by selecting them from a larger batch. Fertilizer (CARBUNA AND, Carbuna AG, Memmingen, Germany as organic fertilizer based on Vinasse and mineral fertilizer Ferty 2 Mega, Hauert MANNA Düngerwerke GmbH, Nürnberg, Germany) was applied five times over the nine weeks of plant growth. The lysimeters were watered by rainfall and, if necessary, by drip irrigation.

2.3. Soil sampling and processing

After nine weeks of plant growth, the lysimeter experiment was harvested in July 2024 (no visible effect of amendment application on plant growth, see Hamburger et al. 2026). The soil was sieved through a 2 mm sieve to remove coarse soil fragments and roots. Since biochar and rock-enhanced biochar have not been crushed prior to application, coarse amendment particles were also removed while sieving. A subsample of the sieved soil material was stored in a 2 ml Eppendorf Tube® at 4 °C until the enzyme assay was conducted (description see chapter 2.5 and appendix chapter 7.3). Another subsample was stored in a plastic bag at 4 °C for further physical and chemical analysis. The remaining sieved soil was air dried.

2.4. Physical and chemical analysis of soil samples

Dried soil samples were used to measure total C and total N contents using an elemental analyzer (Vario Max Cube, Elementar Analysensysteme GmbH, Langenselbold, Germany). Due to the low soil pH of our samples (< 6.5), we consider total C and TOC as equivalent. Available P content was determined using calcium lactate and hydrochloric acid following VDLUFA (1991) and measured using a spectrophotometer (DR5000, Hach Lange GmbH, Düsseldorf, Germany) with a wavelength of 580 nm. Soil pH was determined in 0.01 M $CaCl_2$ solution (soil: $CaCl_2$ solution = 1:2.5) using a pH meter (MP230, Mettler-Toledo GmbH, Gießen, Germany). The electric conductivity (EC) was measured in deionized water (soil: water = 1:2.5) using a conductivity meter (Cond 330i, WTW GmbH, Weilheim, Germany).

The water content (WC) of the fresh samples was determined by weighing the difference between the cooled sample and after drying the sample at 105 °C until constant weight. Mineral N (N_{min}) of the cooled samples was extracted following DIN (2005) using 0.0125 M $CaCl_2$ and the extract was measured using a spectrophotometer (LLG-unispec 4, Lab Logistics Group GmbH, Meckenheim, Germany) for ammonium and using high performance liquid chromatography (1100 HPLC, Agilent Technologies Inc., Santa Clara, California, USA) for nitrate and nitrite. These field-moist samples were also used to determine C_{mic} using the chloroform fumigation extraction (CFE) method after DIN (2011) adapted from Vance et al. (1987). Two times 12.5 g dry weight equivalent per sample were weighed in glass flasks. One of the samples was directly extracted with 50 ml of 0.05 M K_2SO_4 solution to quantify dissolved organic carbon (DOC). The second sample was fumigated with chloroform to lyse microbial cell walls and was afterwards also extracted using K_2SO_4 solution. The extracts were analyzed using a TOC analyzer (TOC-L, Shimadzu Corporation, Kyoto, Japan). To be able to measure the CFE extracts also at an isotopic ratio mass spectrometer, we used 0.05 M K_2SO_4 solution (Werth and Kuzyakov, 2010). The difference between the extracted C contents in fumigated and non-fumigated samples is interpreted as C_{mic}, using an extraction factor k_{EC} of 0.45 (Joergensen, 1996).

2.5. Fluorometric enzyme assays

Enzyme activities were determined as a proxy for nutrient dynamics using fluorogenic substrates (Marx et al., 2001). Four fluorogenic substrates were used associated with either 4-methylumbelliferon (MUF) or 7-amido-4-methylcoumarin (AMC): MUF-ß-D-glucoside (for detection of BG), MUF-N-acetyl-ß-D-glucosidase (for detection of CH), MUF-phosphatase (for detection AP), and L-leucine-AMC-hydrochloride (for detection of LAP).

Homogenized cooled (4 °C) soil samples (0.5 g dry weight equivalent) were weighed in sterile 100 ml glass flasks and 50 ml of sterile water was added. Each sample was sonicated using an ultrasonication probe for two minutes with an output energy of 40 J s^{-1}. A volume of 50 µl of the soil suspensions was pipetted into sterile deep-well plates (Nunc™ F96 MicroWell™ plate, black, 96 well, Thermo Scientific™). Afterwards, 50 µl of MES or TRIZMA buffer (for MUF- and AMC-linked substrates respectively) and 100 µl of substrate solution were added. The use of differently concentrated substrate solutions resulted in final concentrations of 0, 1, 2, 3, 4, 5, 10, and 20 µmol g^{-1} dry soil for MUF-linked substrates and of 0, 1, 2, 3, 5, 10, 20, and 40 µmol g^{-1} dry soil for AMC-linked substrates in the deep-well plates. Three analytical replicates were measured for each sample at each substrate concentration.

For calibration, soil suspensions (50 µl per well) and MES or TRIZMA buffer solutions (150, 140, 130, 100, 70, and 30 µl, respectively) were mixed in deep-well plates with either 10 µM MUF or AMC standards (0, 10, 20, 50, 80, and 120 µl, respectively). Fluorescence of all deep-well plates was measured directly and 120 min after substrate addition (excitation wavelength of 355 nm, emission wavelength of 460 nm) using a microplate reader (Victor^3 1420–05 Multi label Counter, PerkinElmer, USA). A more detailed description of the method can be found in appendix chapter 7.3.

2.6. Data analysis

The kinetic parameters V_{max} and K_m were calculated using the Michaelis Menten equation (Eq. 1; after Michaelis and Menten, 1913), while soil enzyme efficiency K_a was calculated using Eq. 2 (after Ndossi et al., 2020; Xiao et al., 2024):

$$v = (V_{max} * [S]) / (K_m + [S]) \quad (1)$$

$$K_a = V_{max} / K_m \quad (2)$$

where v is the reaction rate of the respective soil enzyme at a certain substrate concentration (nmol MUF/AMC h^{-1} g^{-1} dry soil), V_{max} represents the maximum rate of soil enzyme reaction at saturated substrate concentration at the given temperature (nmol substrate h^{-1} g^{-1} dry soil), K_m is the substrate concentration at ½ V_{max} (µmol g^{-1} dry soil) representing the respective enzyme binding affinity to its specific substrate, *[S]* is the substrate concentration (µM), and K_a is the catalytic enzyme efficiency.

Extracellular enzyme stoichiometry (EES), a proxy for microbial nutrient demand, was calculated as the ratio of C- (BG), N- (LAP), and P-related (AP) enzymes after the concept of Sinsabaugh et al. (2008) following the descriptions of Deng et al. (2019) and Yang et al. (2020):

$$\text{Enzyme } C:N \text{ ratio} = \ln(V_{\max}BG) / \ln(V_{\max}LAP) \quad (3)$$

$$\text{Enzyme } C:P \text{ ratio} = \ln(V_{\max}BG) / \ln(V_{\max}AP) \quad (4)$$

$$\text{Enzyme } N:P \text{ ratio} = \ln(V_{\max}LAP) / \ln(V_{\max}AP) \quad (5)$$

The ratio of the activities of C-, N-, and P-acquiring enzymes is used to assess soil microbial nutrient limitation. While a ratio of C:N:P (lnBG: lnLAP: lnAP) of 1:1:1 represents an equilibrated system, a value > 1 indicates a limitation of the respective nutrient. To have comparable ratios for the five treatments, the ratios were standardized to a C-value of 1. In addition, these ratios can be used to calculate the length and the angle of connecting the respective nutrient ratio in a C:N-to-C:P figure relative to the figure origin (Moorhead et al., 2016; Deng et al., 2019). The vector length indicates the relative C-to-P/N-limitation with an increasing vector length suggesting an increasing C limitation. The vector angle indicates a relative N-to-P-limitation, with a vector angle $< 45^\circ$ representing N limitation and $> 45^\circ$ representing P limitation (Moorhead et al., 2016; Deng et al., 2019). Vector length and angle were calculated after Moorhead et al. (2016):

$$\text{vector length} = \sqrt{(x^2 + y^2)} \quad (6)$$

$$\text{vector angle} = \arctan(x, y) \quad (7)$$

where x is the enzyme C:P ratio and y the enzyme C:N ratio.

To test for significant differences ($p < 0.05$), we used a linear mixed effects (LME) model and a linear model for enzyme kinetics and soil properties, respectively, followed by a Tukey HSD post-hoc test for pairwise comparison. Outliers of v, V_{max}, K_m, K_a, and EES were detected using the Dixon's Q test to check the measurement accuracy and to check the influence of sample and block on measurement results. P-values < 0.1 were in general interpreted as the tendency towards a difference. All calculations and statistical tests were conducted in RStudio (version 4.4.2) using 'outliers' package (Komsta, 2022) to detect outliers, 'lme4' package (Bates et al., 2015) for LME computing, 'multcomp' package (Hothorn et al., 2008) for compact letter display, 'ggplot2' package (Wickham, 2016) for data visualization, and 'ggcorrplot' package (Kassambara, 2023) for correlation matrices.

Differences (%) of amended treatments compared to control were calculated using Eq. 8:

$$\text{difference} = \frac{(value_{control} - value_{amended})}{value_{amended}} * 100 \quad (8)$$

where $value_{control}$ is the measured or calculated value of the control treatment and $value_{amended}$ is the measured or calculated value of the amended treatments (rock powder, biochar, co-application, and co-pyrolysis treatment).

3. Results

3.1. Effect of amendment application on soil properties

The application of biochar-containing amendments (biochar, co-application, and co-pyrolysis treatments) significantly increased the soil C content by up to 69% (Fig. 1 A). The co-application significantly increased N contents by 8%, while neither biochar nor co-pyrolysis treatment altered N contents (Fig. 1 B). Since the increase in C content was more pronounced than the increase in N content, the C:N ratio was significantly increased in the biochar-containing treatments (Fig. 1 C).

The application of biochar-containing amendments significantly increased DOC, C_{mic}, P, pH, and EC compared to control (Fig. 1 D, E, G, H, I). Additionally, all of these soil properties except C_{mic} showed significant differences between the three biochar-containing treatments. The available P content was increased by 125% in biochar treatment compared to the control, followed by the co-application treatment with an increase of 110% (Fig. 1 G). A lower, but still significant increase in P content of 65% was visible in co-pyrolysis treatment compared to control. For pH and EC, their increase was higher in co-application treatment compared to co-pyrolysis treatment (Fig. 1 H, I). The increase in DOC content by 83% was most pronounced in co-pyrolysis treatment and lowest in co-application treatment (47%; Fig. 1 D). For both pH and DOC content the increase following biochar application was not significantly different from both combined amendments (Fig. 1 D, H).

In contrast to the strong effect of biochar-containing amendments, basanite application alone did not alter any of the analyzed soil properties significantly (Fig. 1 A-I). Only the available P content tended to decrease ($p < 0.1$) following basanite application (Fig. 1 G). The only soil property analyzed in this study, which was not influenced by any of the amendments, was N_{min} (Fig. 1 F).

3.2. Effect of amendment application on extracellular enzyme kinetics

Potential enzyme activity V_{max} was generally highest for AP with values up to 24 times higher in all treatments compared to the other enzymes ($p < 0.001$), while LAP tended generally to have the lowest V_{max} ($p < 0.1$; Fig. 2 A-D). The application of biochar-containing amendments strongly influenced V_{max} of all four enzymes. Both biochar and co-application treatment resulted in a significant decrease of V_{max} for AP and CH compared to control by up to 57%. The co-pyrolysis treatment had the smallest influence among the three biochar-containing treatments on V_{max}. The co-pyrolysis treatment significantly decreased V_{max} of AP by 35% compared to control but showed a significantly lower effect compared to biochar treatment. While biochar-containing amendments mainly decreased V_{max} of AP and CH, V_{max} of LAP showed the opposite pattern. Both biochar and co-application doubled V_{max} of LAP compared to control treatment and the co-pyrolysis treatment tended to increase V_{max} ($p < 0.1$) compared to control by 45%. In contrast to the strong effect of biochar-containing amendments, basanite application did not influence V_{max} for all four enzymes compared to the control.

The differences in K_m between enzymes and treatments is less pronounced than the differences between enzyme and treatments we observed in V_{max} (Fig. 2 E-H). The application of biochar decreased K_m of AP by 33% and quadrupled K_m of LAP compared to control, while it did not influence K_m of BG and CH. The co-application increased K_m of BG by 97% compared to control, but had no significant effects on K_m of the AP, CH, and LAP. Both basanite and co-pyrolysis treatments did not alter K_m of any of the enzymes.

In all treatments, AP showed up to 16 times higher enzyme efficiency K_a compared to BG, CH, and LAP (Fig. 2 I-L). Both biochar and co-application significantly decreased K_a of AP and BG by up to 50% and decreased (biochar) or tended to decrease (co-application) K_a of CH by up to 45% compared to control (Fig. 2 I-K). Reflecting the patterns of V_{max}, co-pyrolysis treatment had the smallest influence on K_a of the three biochar-containing amendments (biochar, co-application, and co-pyrolysis treatments). The co-pyrolysis treatment tended to lower the K_a value of BG compared to control ($p < 0.1$), while it did not alter K_a of AP, CH, and LAP. In contrast to AP, BG, and CH, K_a of LAP was not influenced by the application of biochar-containing amendments (Fig. 2 L). Basanite application in general did not significantly influence K_a of any of the studied enzymes.

Soil extracellular enzyme stoichiometric C:N and N:P ratio changed significantly through the application of biochar-containing amendments compared to control, while the C:P ratio was not altered (Fig. 3). The enzyme C:N ratio decreased by up to 42% compared to control (Fig. 3 A), while the enzyme N:P ratio was up to doubled following the application

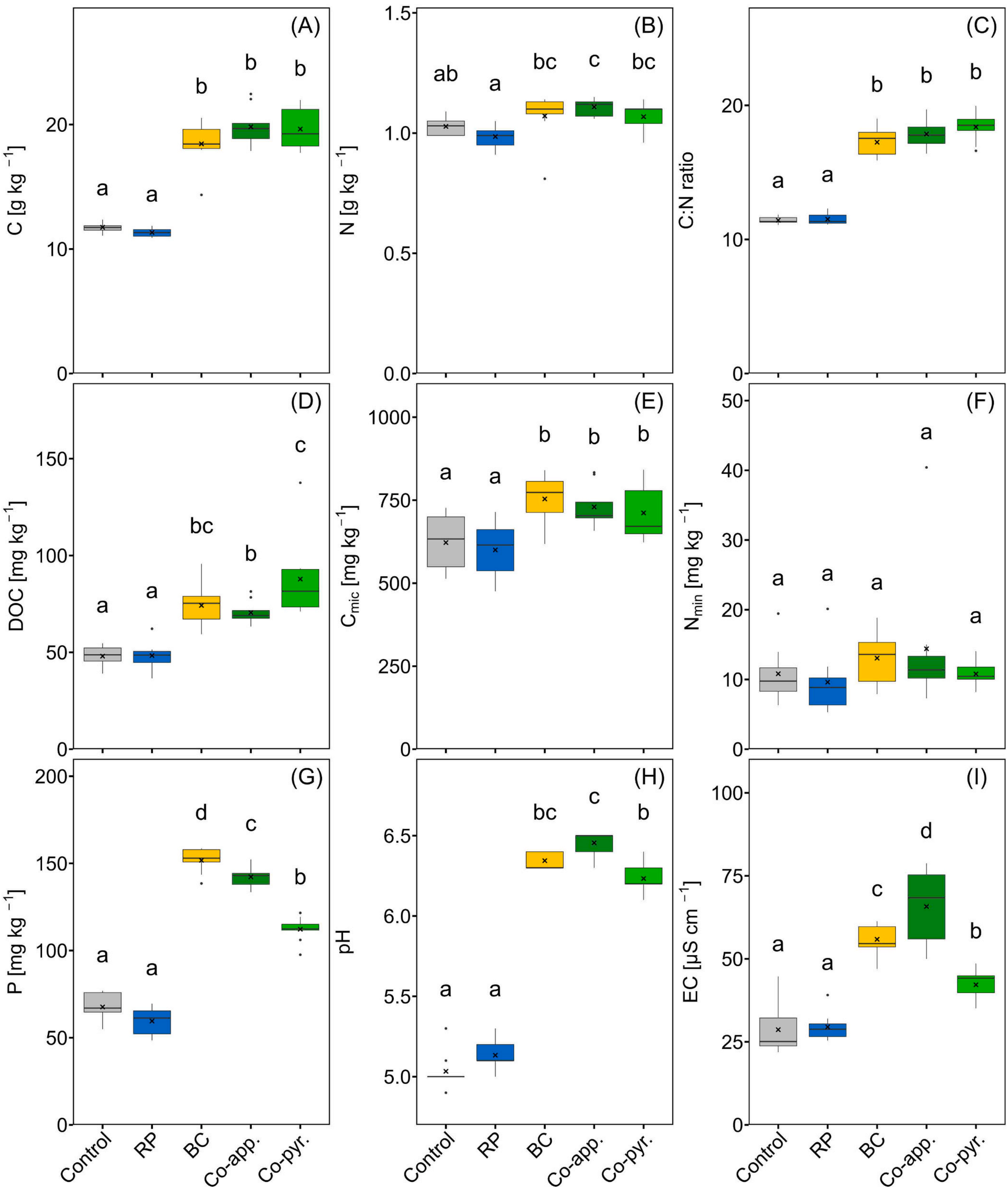

Fig. 1. Total C content (A), total N content (B), C:N ratio (C), dissolved organic carbon (DOC) content (D), microbial biomass C (C_{mic}) content (E), total mineral N (N_{min}) content (F), available P content (G), pH in $CaCl_2$ (H), and electric conductivity (EC) (I) of five treatments of soil with different amendments (n = 9 per treatment). RP = rock powder treatment containing basanite, BC = biochar treatment, Co-app. = co-application treatment, Co-pyr. = co-pyrolysis treatment containing rock-enhanced biochar. Small letters indicate significant differences ($p < 0.05$) between treatments within one soil property.

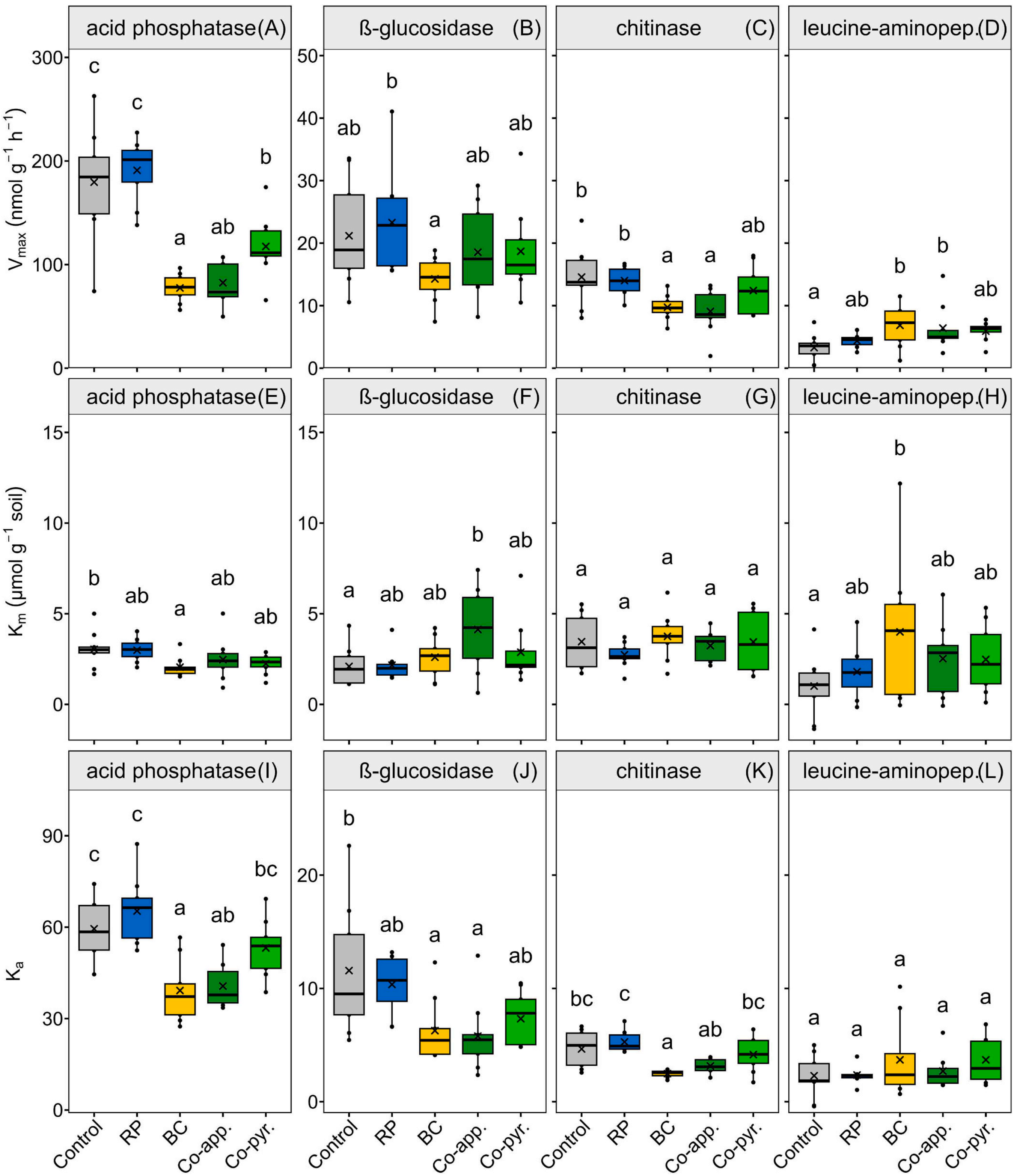

Fig. 2. Potential enzyme activity V_{max} (a-d), enzyme affinity K_m (e-h), and catalytic enzyme efficiency K_a (i-l) of acid phosphatase (AP), ß-glucosidase (BG), chitinase (CH), and leucine-aminopeptidase (LAP) in five treatments of soil with different amendments (n = 9 per treatment). RP = rock powder treatment containing basanite, BC = biochar treatment, Co-app. = co-application treatment, Co-pyr. = co-pyrolysis treatment containing rock-enhanced biochar. Small letters indicate significant differences ($p < 0.05$) between treatments within one parameter and enzyme. To increase readability, the y-axis of BG, CH, and LAP for V_{max} and K_a have a higher resolution than those of AP.

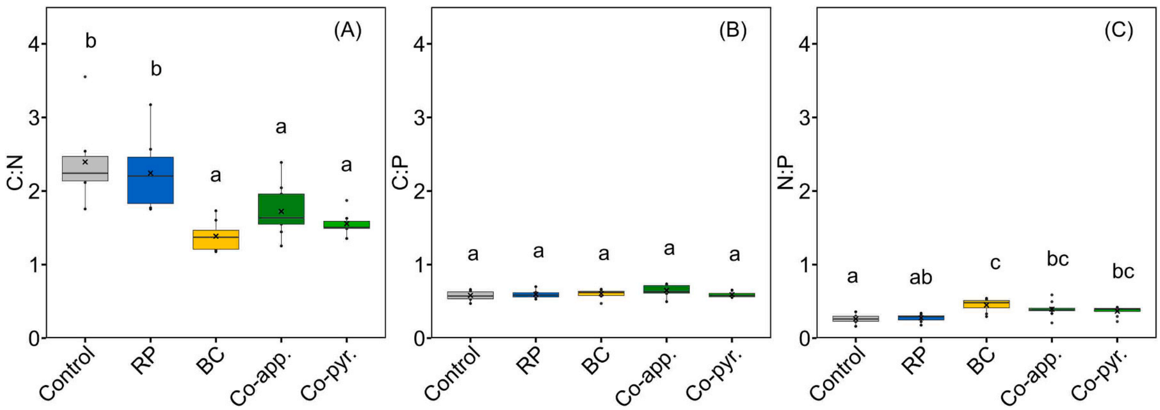

Fig. 3. Extracellular enzyme stoichiometry (EES) ratios of C:N (ln(BG): ln(LAP)) (a), C:P (ln(BG): ln(AP)) (b), and N:P (ln(LAP): ln(AP)) (c) in five treatments of soil with different amendments (n = 9 per treatment). ln(BG) = ln of V_{max} of ß-glucosidase, ln(LAP) = ln of V_{max} of leucine-aminopeptidase, ln(AP) = ln of V_{max} of acid phosphatase. RP = rock powder treatment containing basanite, BC = biochar treatment, Co-app. = co-application treatment, Co-pyr. = co-pyrolysis treatment containing rock-enhanced biochar. Small letters indicate significant differences ($p < 0.05$) between treatments within one stoichiometric ratio.

of biochar-containing amendments (Fig. 3 C). Based on those C:N, C:P, and N:P ratios, the combined enzymatic C:N:P ratios reflected the strong influence of biochar-containing amendments on N dynamics. The control treatment had an enzymatic C:N:P ratio of 1:0.28:1.74. Biochar application had the strongest influence and resulted in an enzymatic C:N:P ratio of 1:0.66:1.67, followed by co-pyrolysis and co-application treatments with enzymatic C:N:P ratios of 1:0.62:1.59 and 1:0.60:1.56, respectively. Basanite application did neither alter EES nor the enzymatic C:N:P ratio significantly compared to control.

The control treatment had a calculated vector length of 2.5 ± 0.5 and an angle of 76.4° ± 3.4° (Fig. 4). The application of biochar-containing amendments resulted in a decrease in vector length and angle, most pronounced in the biochar treatment with a calculated vector length of 1.5 ± 0.2 and an angle of 66.4° ± 4.5°. Basanite application did neither alter vector length nor angle compared to control.

3.3. Correlation between soil properties and enzyme kinetics

The enzyme kinetics (V_{max}, K_m, K_a) and analyzed soil properties showed strong significant correlations for all four enzymes. For AP, enzyme kinetics showed strong negative correlations with all investigated soil properties across all treatments (Fig. A.1). The effects of C, N, P, and C_{mic} content as well as pH and EC were especially pronounced on

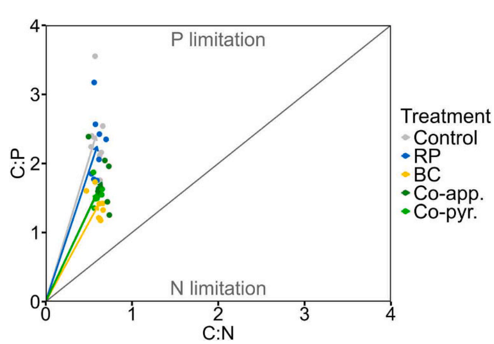

Fig. 4. Relationship between ratios of C:N (ln(BG):ln(LAP)) and C:P (ln(BG):ln(AP)) in five treatments of soil with different amendments (n = 9 per treatment) with arrows indicating the treatment-specific vector length from the figure origin. The angle between the vector and the x axis represents the vector angle. ln(BG) = ln of V_{max} of ß-glucosidase, ln(LAP) = ln of V_{max} of leucine-aminopeptidase, ln(AP) = ln of V_{max} of acid phosphatase. RP = rock powder treatment containing basanite, BC = biochar treatment, Co-app. = co-application treatment, Co-pyr. = co-pyrolysis treatment containing rock-enhanced biochar.

AP's V_{max} but were often also significant in K_m and K_a. Similarly to AP, V_{max} and K_a (but not K_m) of CH showed negative but less pronounced correlations with C, P, and C_{mic} content as well as pH and EC (Fig. A.2). The enzyme kinetics of CH did not correlate significantly with N_{min} and N contents. The enzyme kinetics of BG showed several negative correlations the analyzed soil properties, such as DOC and C_{mic} content as well as pH and P content (Fig. A.3). In contrast to AP, BG, and CH, the enzyme kinetics of LAP showed solely positive correlations with the analyzed soil properties (Fig. A.4). Both V_{max} and K_m of LAP correlated positively with C, N, and P content as well as C:N ratio and soil pH. Catalytic enzyme efficiency K_a of LAP correlated positively with only DOC content.

4. Discussion

4.1. Influence of amendments on soil C, pH, and nutrients

The application of all three biochar-containing amendments (biochar, co-application, and co-pyrolysis treatments) increased C content, C:N ratio, and C_{mic} content equally strong within our nine-week experiment. Consequently, synergistic or diminishing effects of rock powder on those soil properties were absent in both combined applications (co-application and co-pyrolysis treatments). Increased C content (Gross et al., 2021; Chagas et al., 2022; Wang et al., 2025a), C:N ratio (Ding et al., 2023), and C_{mic} content (Lehmann et al., 2011; Liu et al., 2015; Buss et al., 2021; Chagas et al., 2022) following biochar application align with the results of former studies. Even though amendment particles > 2 mm were removed in our study, a significant increase in C content and C:N was visible, mainly resulting from the high content of stable C in biochar (Joseph et al., 2010; Gross et al., 2021; Qiu et al., 2023). The observed enhancement of C_{mic} in our study likely reflects improved microbial habitat and growth conditions due to the application of biochar-containing amendments (Ghodszad et al., 2021). These are probably driven by increases in soil pH, nutrient and water retention capacity, and labile C availability (Van Zwieten et al., 2010; Liu et al., 2015), e.g. from increased DOC content (Azeem et al., 2023; Chen et al., 2024).

Biochar application is generally known to result in increased soil pH (Dai et al., 2017; Buss et al., 2018) and to potentially increase EC (Chintala et al., 2014; Hu et al., 2025). The observed increases in soil pH and EC in our study were most pronounced following the co-application of biochar and basanite. This suggests a synergistic effect likely driven by the combined liming and ionic contributions of both amendments. The application of the co-pyrolyzed rock-enhanced biochar showed a less pronounced effect compared to co-application. This attenuation may be attributed to altered mineral availability or reduced soluble salt content resulting from thermal transformation during co-pyrolysis.

By modifying soil pH (Shepherd et al., 2017; Ghodszad et al., 2021) or by increasing cation exchange capacity (CEC; Liang et al., 2006; Kareem et al., 2025), biochar application can increase P availability and reduce P leaching. Additionally, biochar application can increase available P content in soils (Jin et al., 2016; Glaser and Lehr, 2019; Wang et al., 2025a) from the dissolution of biochar ash which contains P_2O_5 that is released into the soil over time (Ghodszad et al., 2021; Buss et al., 2022). These effects can be short-, mid-, or long-term (Glaser and Lehr, 2019), depending strongly on soil and biochar properties (Ghodszad et al., 2021). The strong correlation between P content and soil pH in our study highlights the indirect influence of biochar-containing amendment applications on P availability via pH increase. However, the pH increase was similar in biochar and co-application, while the increase in available P content was most pronounced following single biochar application. The reduced increase in P availability following combined applications compared to single biochar could result from reduced biochar ash dissolution, possibly due to clogged biochar pores, or reduced CEC and thus reduced retention of fertilizer P. The pelletizing of the rock-enhanced biochar prior to pyrolysis could explain the even less pronounced increase in available P compared to co-application, due to compressing biomass pores and thus reducing specific surface area. Building on these findings, future work assessing amendment characteristics, such as specific surface area, could deepen our understanding of the mechanisms involved. A reduced ash dissolution in the short-term might lead to a more stable P supply in the long-term following combined application (Lammirato et al., 2011; Buss et al., 2022).

The application of biochar to sandy soils can have diverse positive and negative impacts on content, retention, and availability of N_{min} (Ahmad et al., 2021; Hematimatin et al., 2024). In our study, the content of N_{min} was neither increased nor reduced by the application of the biochar-containing amendments. Since the application of these amendments significantly reduced nitrate leaching (Hamburger et al., 2026), nitrate retention was improved and suggests with the constant N_{min} content an increased microbial uptake of N_{min} following the application of the biochar-containing amendments.

In contrast to the biochar-containing amendments, the single application of basanite did not influence any of the analyzed soil properties during the nine weeks of plant growth. In contrast, other studies discovered a variety of effects of silicate rock powder application on soil properties, such as altered TOC (Amoakwah et al., 2023; Buss et al., 2023; Sokol et al., 2024; Xu et al., 2024b), C_{mic} (von Mersi et al., 1992; Reis et al., 2024; Sokol et al., 2024), and nutrient contents (Amann et al., 2020; Guo et al., 2023; Wang et al., 2025b) as well as increased soil pH (Abdalqadir et al., 2024; Beerling et al., 2025; Medeiros et al., 2025). These effects of ERW are often visible in the long-term (Swoboda et al., 2022; Dupla et al., 2024), possibly explaining the missing effects of basanite application in our nine-weeks study.

Our results partly confirm our hypothesis that the combined application of biochar and basanite improved soil properties relevant to microbial activity. Key soil properties, such as C and P content, C:N ratio, and C_{mic}, increased significantly following combined application compared to control, indicating positive effects. The observed changes were mainly driven by the biochar component, while potential contributions of basanite may require more time to become effective. Nevertheless, the pronounced changes in pH and EC under co-application compared to co-pyrolysis suggest potential for synergies between biochar and basanite without a significant benefit of combined pyrolysis.

4.2. *Influence of amendments on extracellular enzyme kinetics*

All treatments showed, despite the fertilization, a P limitation and, possibly due to the fertilization, a generally low N demand. This is indicated by the high V_{max} of AP, low V_{max} of LAP, vector angles > 45°, and enzymatic C:N:P ratios with P-values > 1 and N-values < 1 (von Mersi et al., 1992; Allison et al., 2007; Moorhead et al., 2016). The application of biochar-containing amendments seemed to induce a shift in microbial nutrient demand. The decrease in V_{max} of AP is consistent with the observed increase in available P. This improved P availability, potentially further enhanced by the pH increase (Swoboda et al., 2022; Beerling et al., 2025), allowed the microorganisms to down-regulate the production of AP (Sinsabaugh et al., 2008; Allison et al., 2011). Simultaneously, the increased V_{max} of LAP indicates an enhanced demand for N, likely driven by the widened soil C:N ratio and the adsorption of N_{min} (Clough et al., 2013) following the application of biochar-containing amendments. This increases the relative stoichiometric imbalance between C and N from the microbial perspective, which can stimulate investment in N-acquiring enzymes such as LAP (Sinsabaugh et al., 2008; Allison et al., 2011) and strengthen the microbial community involved in N cycling (Anderson et al., 2011). Even though P remained the limiting nutrient for microorganisms, the application of biochar-containing amendments seemed to shift the system towards a more balanced nutrient demand with a relative increase in N demand. The potential enzyme activity V_{max} of AP, CH, and LAP following the application of co-pyrolyzed rock-enhanced biochar was similar to that of control, while both biochar and co-application significantly altered those potential enzyme activities. This can likely be explained by the strong correlation of V_{max} with available P and soil pH, which were also less strongly increased with rock-enhanced biochar application. Despite that, the similar enzymatic C:N:P ratios following all three biochar-containing amendments implies that the rock-enhanced biochar application probably resulted in an equally strong balancing of the nutrient demand as biochar and co-application.

The potential activity V_{max} of the C-cycle-related BG was, contrary to our hypothesis, not affected by the application of biochar-containing amendments. In contrast, several other studies reported increased V_{max} of BG following biochar application (Halmi and Simarani, 2021; Jin et al., 2024). However, biochar produced at high temperatures (> 500 °C) has been observed to have minimal or even inhibiting effects on BG activity (Jin et al., 2024; Yang et al., 2024), potentially due to greater porosity and surface area (Liao et al., 2022). The application of biochar might relocate both C and microorganisms onto biochar surfaces, which may improve microbial efficiency and reduce the need for BG release (Lehmann et al., 2011). Bamminger et al. (2014) interpreted an increase in potential BG activity as a result of insufficient C supply from biochar to support microbial growth. Since we observed an increased C_{mic} content and the calculated vector lengths did not indicate a C limitation following biochar-containing amendment application, the labile biochar part must have provided sufficient C to sustain microbial growth. While our approach provides valuable initial insights into effect of our amendments on C-cycle dynamics, the focus on BG may only reflect part of the microbial response. Including additional C-cycling enzymes, such as β-xylosidase or β-cellobiohydrolase, in future studies could help to broaden the understanding of enzymatic activity patterns in response to combined application of biochars and silicate rock powder (Loeppmann et al., 2016).

In contrast to V_{max}, the enzyme affinity K_m of all four enzymes was barely influenced by amendment application. Little is known about the influence of biochar and basanite application of enzyme affinity K_m, but our results indicate robustness against the influence of both amendments. Since K_m has rarely been influenced by the amendments, catalytic enzyme efficiency K_a as the quotient of V_{max} and K_m showed similar patterns as V_{max}. Both biochar and co-application may result in a reduced catalytic enzyme efficiency K_a of AP, BG, and CH, probably due to a strong increase in P and C supply.

The basanite treatment did neither improve nor impair enzyme kinetics and EES, which makes basanite a promising CDR method without a harmful impact on enzymes and microbial processes. Until now, there have been only a few studies investigating the influence of silicate rock powder on soil microbial processes in planted systems. These studies have inconsistent results ranging from increased to decreased V_{max} of different enzymes, strongly depending on soil and rock powder properties as well as the analyzed enzyme (von Mersi et al., 1992; Li and Dong, 2013; Reis et al., 2024; Wang et al., 2025b). The enzyme kinetics in our study strongly correlated with soil properties, such as nutrient contents and soil pH, which determine nutrient availability and thus affect enzyme activities (Sinsabaugh et al., 2008). Since those parameters were not altered by basanite applied in our study – potentially due to low amounts or insufficient time to weather –, a missing effect on enzyme kinetics, EES, and vector length and angle is not surprising. Reis et al. (2024) showed a significant decrease in AP activity first occurring four months after basalt application. This long-term decrease in AP activity was explained by the low but apparently sufficient content of P_2O_5 in the basalt to supply microorganisms with P, thereby reducing the need for AP release (Reis et al., 2024). Since our basanite had similar P_2O_5 contents (~0.6 wt%) but did not alter AP activities, this supports the impression of low basanite weathering rates in our experiment. In the long-term, we would expect basanite application to have an impact on enzyme kinetics, especially on AP.

Enzyme kinetics and thus enzyme-based nutrient limitation indices, including EES and vector analysis, provide a valuable framework for comparing microbial nutrient demand. However, these indices are influenced not only by microbial stoichiometry, but also by abiotic factors such as enzyme adsorption to biochar surfaces (Lehmann et al., 2011; Lammirato et al., 2011) and soil pH and temperature (Sinsabaugh et al., 2008; Moorhead et al., 2016). The threshold angle of 45° for distinguishing N from P limitation is an established proxy (von Mersi et al., 1992; Allison et al., 2007; Moorhead et al., 2016), but may oversimplify the complex interactions between soils and microbes. Nonetheless, the combined use of enzyme kinetics and stoichiometric ratios applied in this study provides valuable first insights into the effects of single versus combined amendment applications on nutrient dynamics, and future work should complement this approach focusing on the microbial community to further disentangle amendment-specific effects.

5. Conclusions

Our experiment, conducted on a sandy agricultural soil, provides an important first step toward understanding effects of the single and combined applications of biochar and basanite on soil properties and microbial processes during a nine-week experiment including plants. The results partly support our hypotheses and reveal distinct short-term responses depending on the applied amendment. Basanite application alone showed no significant effects, likely due to limited weathering over the short experimental duration, which constrained the release of nutrients from the mineral phase. To be able to assess the influence of silicate rock powder application of soil properties and microbial processes, long-term studies are necessary. Nonetheless, basanite application caused no negative impacts within our nine-week experiment, supporting its potential as a safe and promising long-term amendment for CDR and soil improvement.

The combination effect of biochar and basanite was primarily driven by biochar, with co-pyrolyzed rock-enhanced biochar and co-application of biochar and basanite resembling the response of single biochar application. These three biochar-containing amendments significantly improved soil properties, such as soil pH, available P, and C_{mic}, and altered extracellular enzyme kinetics and nutrient stoichiometry. All biochar-containing treatments increased soil C content, C:N ratio, and C_{mic} to a similar extent. While single biochar application enhanced short-term P availability, co-application and especially co-pyrolysis treatments may offer a more sustained long-term P release. Co-application led to the greatest increases in soil N content, pH, and EC, suggesting synergistic effects between biochar and basanite on soil properties within weeks, with the potential to combine the CDR effects of both amendments in the long-term.

Following the application of single biochar and co-application of both amendments to our sandy soil, potential enzyme activity V_{max} of AP, BG, and CH decreased, but increased for LAP. The application of co-pyrolyzed rock-enhanced mainly did not alter V_{max} compared to control, likely due to less pronounced increases in pH and available P. The enzymatic C:N:P ratio varied, indicating a shift from a pure P limitation in the unamended soil to a more balanced nutrient demand in biochar-containing treatments, with increased relative N demand. When applied to agricultural soils, the biochar-containing amendments improved P availability, but could cause long-term N-limitation if not balanced by sufficient N supply.

Funding

This study was conducted as a part of the PyMiCCS project (Pyrogenic carbon and carbonating Minerals for enhanced plant growth and Carbon Capture and Storage) as part of the CDRterra consortium and was funded by the German Federal Ministry of Research, Technology and Space (BMFTR, FKZ: 01LS2109A and 01LS2109C). The datasets generated during the current study are available at https://doi.org/10.25592/uhhfdm.18032.

CRediT authorship contribution statement

Maria Ansari: Writing – original draft, Visualization, Investigation, Formal analysis, Conceptualization. **Stock Svenja C.:** Writing – review & editing, Methodology. **Michaela A. Dippold:** Writing – review & editing, Resources. **Susanne E. Hamburger:** Writing – review & editing, Resources. **Claudia I. Kammann:** Writing – review & editing, Resources, Funding acquisition. **Johannes Meyer zu Drewer:** Resources. **Nikolas Hagemann:** Writing – review & editing, Resources, Funding acquisition. **Annette Eschenbach:** Writing – review & editing, Supervision, Resources, Funding acquisition. **Joscha N. Becker:** Writing – review & editing, Supervision, Funding acquisition, Conceptualization.

Declaration of Competing Interest

The authors declare that they have no known competing financial interests or personal relationships that could have appeared to influence the work reported in this paper.

Acknowledgements

The authors thank the German Federal Ministry of Research, Technology and Space (BMFTR) for funding this study as part of the PyMiCCS project. Furthermore, we thank Sumita Rui and Josephine Krechel for assisting during sampling as well as Deborah Harms and Annika Naumann for support during lab work. We particularly thank Moses Ngugi, Elisa Karina Albrecht, and Callum Banfield for support during the fluorometric enzyme assays.

Appendix

Basanite powder properties

The chemical composition of the rock powder (Table A.1) was analyzed using X-ray fluorescence (XRF) at the Mineralogical Institute, University of

Hamburg, while the mineralogical composition was determined by Qmineral using X-ray diffraction (XRD), as described in Vorrath et al. *under review*. Following the classification of volcanic rocks by Streckeisen (1980) or Le Bas et al. (1986), this rock can be classified as a basanite. The basanite was obtained from Rheinische Provinzial-Basalt- u. Lavawerke, Sinzig, Germany.

Table A.1

Table A.1
Main compounds, trace elements, mineral composition and grain size of used basanite powder *Eifelgold*

Main compounds	[wt%]	Trace Elements	[ppm]	Mineralogy	[wt%]	Grain size [μm]	[wt%]
SiO_2	43.86	As	bdl	Clinopyroxene	44.4	> 300	0.00
TiO_2	2.79	Ba	1026	Plagioclase	15.5	300–250	0.13
Al_2O_3	14.15	Bi	bdl	Nepheline	11.2	250–210	0.17
Fe_2O_3	11.28	Ce	104	Leucite	9.9	210–180	0.14
MnO	0.18	Co	51	Olivine	6.3	180–150	0.26
MgO	8.21	Cr	53	2:1 layer silicates	5.1	150–120	1.20
CaO	11.63	Cu	66	Hematite	3.1	120–100	2.87
Na_2O	3.26	Ga	17	Spinel-type minerals	1.9	100–86	4.17
K_2O	3.35	La	52	Apatite	1.1	86–74	5.67
P_2O_5	0.6	Nb	52	Analcime	0.9	74–62	8.13
SO_3	bdl	Nd	28	Quartz	0.7	62–52	8.89
LOI	0.44	Ni	124			52–44	8.50
Sum	*99.74*	Pb	5			44–36	9.63
		Rb	86			36–30	7.86
		Sc	22			30–26	5.50
		Sr	882			26–22	5.64
		Th	8			22–18	5.72
		U	3			18–0.5	25.52
		V	302				
		Y	24				
		Zn	90				
		Zr	271				

bdl = below detection limit; LOI = loss on ignition.

Randomized complete block design

Fig. A.1

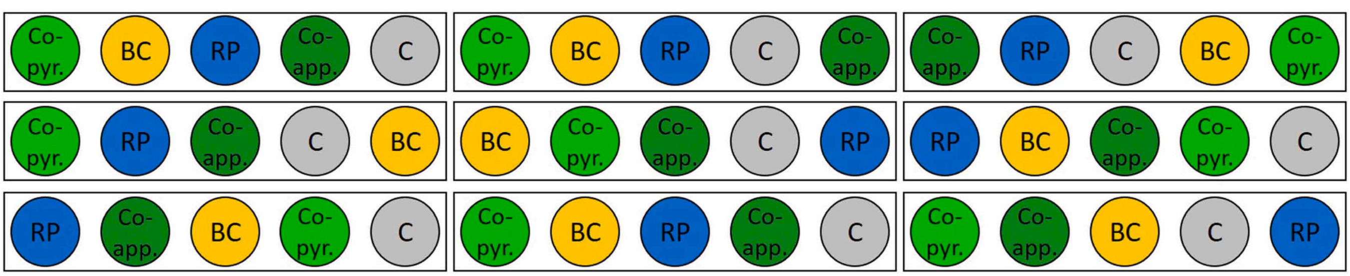

Fig. A.1. Visualization of randomized complete block design of lysimeter experiment. Squares represent blocks, circles represent lysimeters. C = control treatment, RP = rock powder treatment containing basanite, BC = biochar treatment, Co-app. = co-application treatment, Co-pyr. = co-pyrolysis treatment containing rock-enhanced biochar

Fluorometric enzyme assay – method description

All equipment was sterilized before usage. Four fluorogenic substrates were used associated with either 4-methylumbelliferon (MUF) or 7-amido-4-methylcoumarin (AMC): MUF-ß-D-glucoside (for detection of BG), MUF-N-acetyl-ß-D-glucosidase (for detection of CH), MUF-phosphatase (for detection AP), and L-leucine-AMC-hydrochloride (for detection of LAP). This fluorogenic method is based on the liberation of fluorescent MUF or AMC once the associated substrate is used. MUF-ß-D-glucoside, MUF-N-acetyl-ß-D-glucosidase, and L-leucine-AMC-hydrochloride were purchased as crystalline material from Sigma Aldrich (Steinheim, Germany), while MUF-phosphatase was purchased as crystalline material from abcr GmbH (Karlsruhe, Germany).

Two sterile buffer solutions were prepared using sterile water. The 0.1 M MES buffer (from 20.673 g of 4-Morpholineethanesulfonic acid hemi-sodium salt in 1000 ml of sterile water; Sigma Aldrich) was prepared for MUF-based substrates and the 0.05 M TRIZMA buffer (from 0.985 g of Trizma® base and 2.66 g of Trizma® hydrochloride with 500 ml of sterile water; Sigma Aldrich) was prepared for the AMC-based substrate. For preparing 10 mM substrate stock solutions, the crystalline substrates were dissolved in dimethyl sulfoxide and sterile water. These stock solutions were diluted with the respective buffer solutions MES or TRIZMA to reach the desired substrate concentrations for the enzyme assay. For MUF-ß-D-glucoside, MUF-N-acetyl-ß-D-glucosidase, and L-leucine-AMC-hydrochloride, these concentrations were 0, 10, 20, 30, 40, 50, 100, and 200 μM. After a first check of AP enzyme activities, we decided to use higher substrate concentrations of 0, 10, 20, 30, 50, 100, 200, and 400 μM for MUF-phosphatase.

To prepare the soil suspension, homogenized samples of cooled (4 °C) soil were used. An equivalent to 0.5 g of dry soil was weighed in a respective glass bottle and 50 ml of sterile water was added. Each sample was sonicated for 2 min with an output energy of 40 J s^{-1}. A volume of 50 μl of the soil suspension were pipetted into sterile deep-well plates (Nunc™ F96 MicroWell™ plate, black, 96 well, Thermo Scientific™) and 50 μl of MES or TRIZMA buffer as well as 100 μl of substrate solution were added. The use of differently concentrated substrate solutions resulted in a gradient of concentrations within a deep-well plate. For MUF-ß-D-glucoside, MUF-N-acetyl-ß-D-glucosidase, and L-leucine-AMC-hydrochloride, these final concentrations were 0, 1, 2, 3, 4, 5, 10, and 20 μmol g^{-1} dry soil, respectively. For MUF-phosphatase this resulted in final substrate concentrations of 0, 1, 2, 3, 5, 10, 20, and 40 μmol g^{-1} dry soil.

For calibration purposes, standard solutions MUF and AMC were used. The 10 mM standard stock solutions were made by dissolving 0.1762 g of MUF or 0.0875 g of AMC, respectively, in 50 ml of methanol and 50 ml of sterile water. For the 10 μM working solutions, the stock solutions were diluted with MES buffer for MUF and TRIZMA buffer for AMC. For the determination of background fluorescence or quenching effects, soil suspensions (50 μl per well) and MES or TRIZMA buffer solutions (150, 140, 130, 100, 70, and 30 μl, respectively) were mixed with either 10 μM MUF or AMC standards (0, 10, 20, 50, 80, and 120 μl, respectively). These soil suspensions were made of a mix out of the nine replicates per treatment.

Fluorescence of the solution in the deep-well plates was measured after 0, 30, 60, and 120 min (excitation wavelength of 355 nm, emission wavelength of 460 nm) using a microplate reader (Victor[3] 1420–05 Multi label Counter, PerkinElmer, USA). During the experiment, the deep-well plates remained at 22 °C. Before each reading of the plate in the microplate reader, the respective plate was shaken carefully. The soil enzyme activity was quantified by comparing with the plates containing the standard solutions.

Correlation matrixes

Fig. A.2, Fig. A.3, Fig. A.4, Fig. A.5

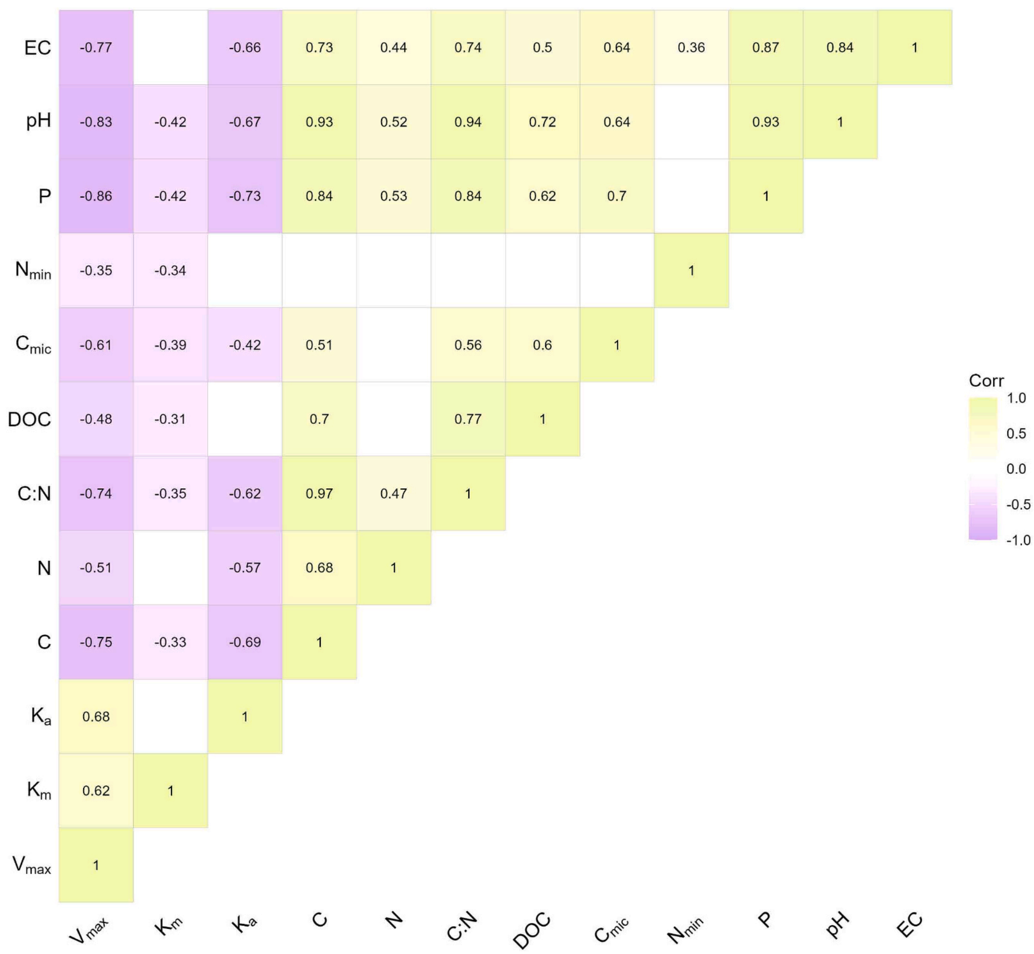

Fig. A.2. Correlation matrix of soil properties and extracellular enzyme kinetics of acid phosphatase (AP). Only significant correlations ($p < 0.05$) are shown. V_{max} = potential enzyme activity [nmol h^{-1} g^{-1} dry soil], K_m = enzyme affinity [μmol g^{-1} dry soil], K_a = catalytic enzyme efficiency, C = total C content [g kg^{-1}], N = total N content [g kg^{-1}], C:N = total carbon to total N ratio, DOC = dissolved organic C content [mg kg^{-1}], C_{mic} = microbial biomass C content [mg kg^{-1}], N_{min} = mineral N content [mg kg^{-1}], P = available P content [mg kg^{-1}], pH = pH value in $CaCl_2$, EC = electric conductivity [μS cm^{-1}]

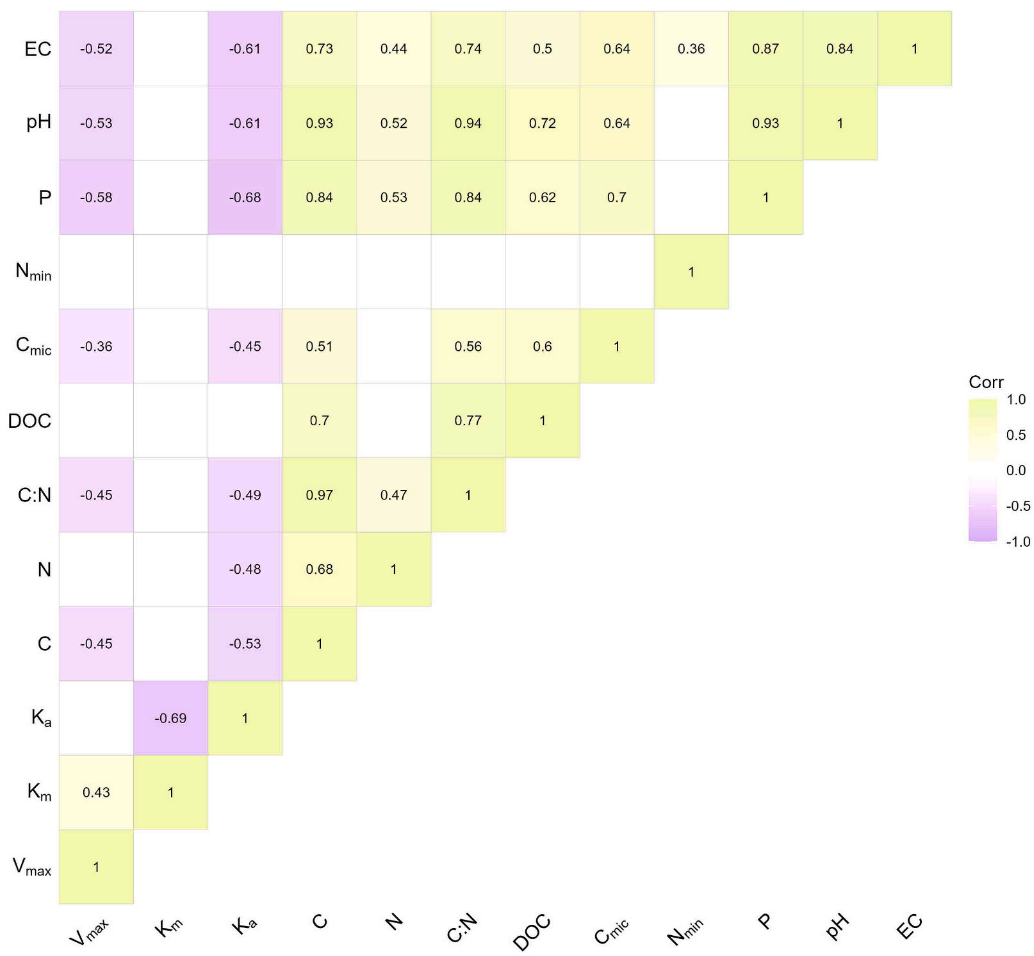

Fig. A.3. Correlation matrix of soil properties and extracellular enzyme kinetics of chitinase (CH). Only significant correlations ($p < 0.05$) are shown. V_{max} = potential enzyme activity [nmol h^{-1} g^{-1} dry soil], K_m = enzyme affinity [μmol g^{-1} dry soil], K_a = catalytic enzyme efficiency, C = total C content [g kg^{-1}], N = total N content [g kg^{-1}], C:N = total carbon to total N ratio, DOC = dissolved organic C content [mg kg^{-1}], C_{mic} = microbial biomass C content [mg kg^{-1}], N_{min} = mineral N content [mg kg^{-1}], P = available P content [mg kg^{-1}], pH = pH value in $CaCl_2$, EC = electric conductivity [μS cm^{-1}]

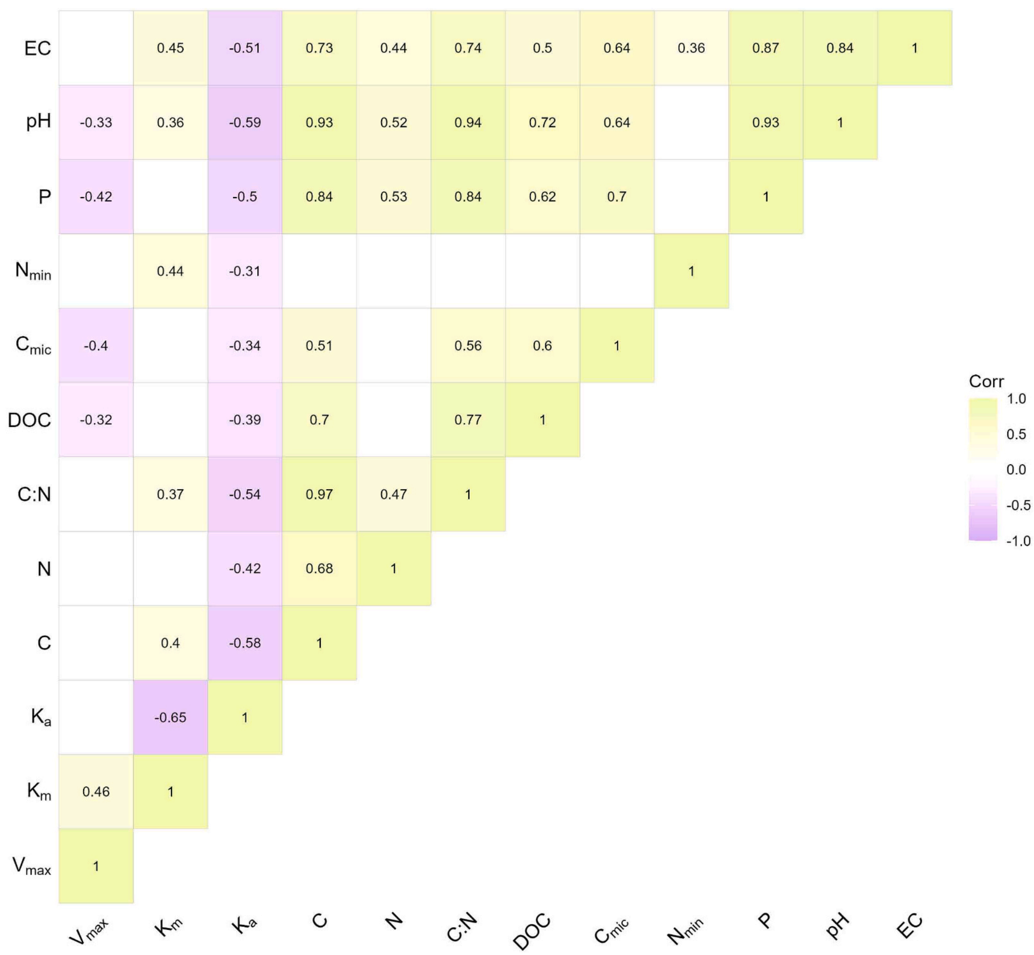

Fig. A.4. Correlation matrix of soil properties and extracellular enzyme kinetics of ß-glucosidase (BG). Only significant correlations ($p < 0.05$) are shown. V_{max} = potential enzyme activity [nmol h^{-1} g^{-1} dry soil], K_m = enzyme affinity [μmol g^{-1} dry soil], K_a = catalytic enzyme efficiency, C = total C content [g kg^{-1}], N = total N content [g kg^{-1}], C:N = total carbon to total N ratio, DOC = dissolved organic C content [mg kg^{-1}], C_{mic} = microbial biomass C content [mg kg^{-1}], N_{min} = mineral N content [mg kg^{-1}], P = available P content [mg kg^{-1}], pH = pH value in $CaCl_2$, EC = electric conductivity [μS cm^{-1}]

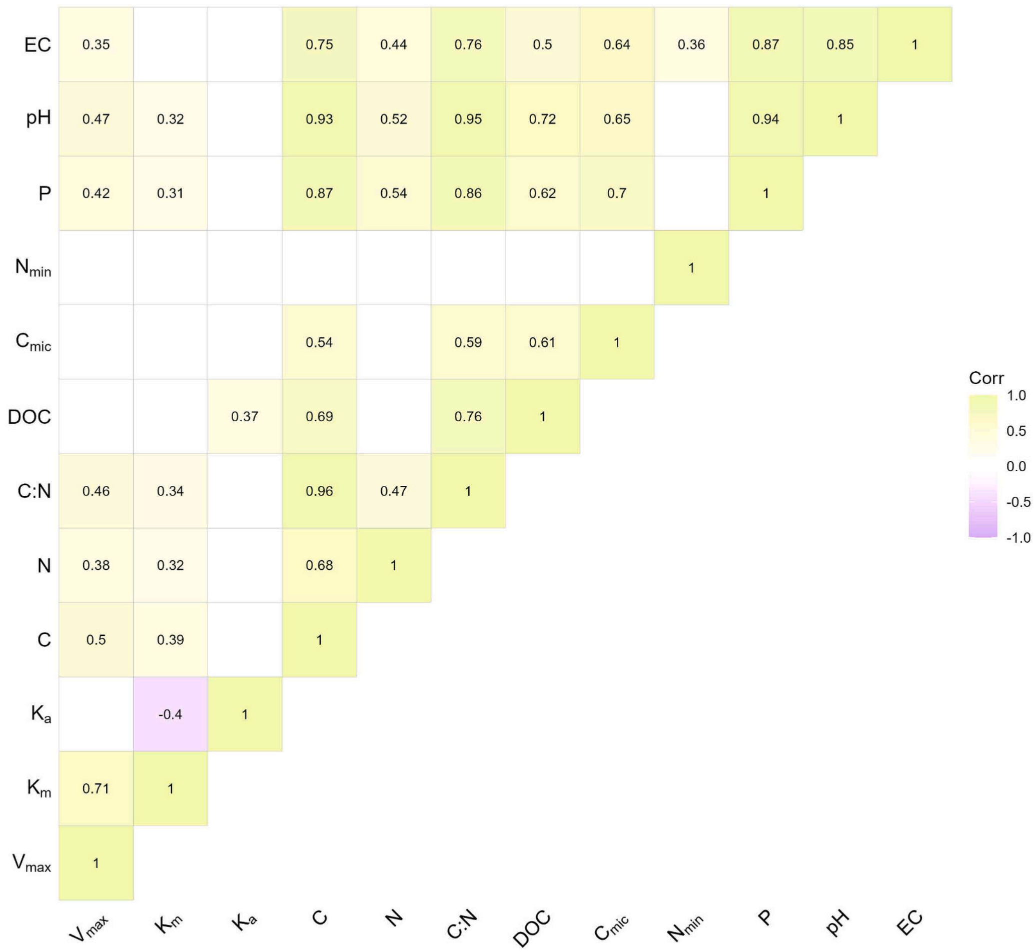

Fig. A.5. Correlation matrix of soil properties and extracellular enzyme kinetics of leucine-aminopeptidase (LAP). Only significant correlations ($p < 0.05$) are shown. V_{max} = potential enzyme activity [nmol h^{-1} g^{-1} dry soil], K_m = enzyme affinity [μmol g^{-1} dry soil], K_a = catalytic enzyme efficiency, C = total C content [g kg^{-1}], N = total N content [g kg^{-1}], C:N = total carbon to total N ratio, DOC = dissolved organic C content [mg kg^{-1}], C_{mic} = microbial biomass C content [mg kg^{-1}], N_{min} = mineral N content [mg kg^{-1}], P = available P content [mg kg^{-1}], pH = pH value in $CaCl_2$, EC = electric conductivity [μS cm^{-1}]

Data availability

Data will be made available on request.

References

Abdalqadir, M., Hughes, D., Rezaei Gomari, S., Rafiq, U., 2024. A state of the art of review on factors affecting the enhanced weathering in agricultural soil: strategies for carbon sequestration and climate mitigation. Environ. Sci. Pollut. R. https://doi.org/10.1007/s11356-024-32498-5.

Ahmad, Z., Mosa, A., Zhan, L., Gao, B., 2021. Biochar modulates mineral nitrogen dynamics in soil and terrestrial ecosystems: a critical review. Chemosphere 278, 130378. https://doi.org/10.1016/j.chemosphere.2021.130378.

Allen, R.L., 1847. A Brief Compend of American Agriculture. University of California, Oakland, California, USA.

Allison, S.D., 2006. Soil minerals and humic acids alter enzyme stability: implications for ecosystem processes. Biogeochemistry 81, 361–373. https://doi.org/10.1007/s10533-006-9046-2.

Allison, S.D., Gartner, T.B., Holland, K., Weintraub, M., Sinsabaugh, R.L., 2007. Soil enzymes: Linking proteomics and ecological processes. In: Hurst, C.J., Crawford, R. L., Garland, J.L., Lipson, D.A., Mills, A.L., Stetzenbach, L.D. (Eds.), Manual of environmental microbiology. ASM Press, pp. 704–711.

Allison, S.D., Weintraub, M.N., Gartner, T.B., Waldrop, M.P., 2011. Evolutionary-economic principles as regulators of soil enzyme production and ecosystem function. In: Shukla, G., Varma, A. (Eds.), Soil Enzymology. Springer Berlin Heidelberg, Berlin, Heidelberg, pp. 229–243.

Amann, T., Hartmann, J., 2019. Ideas and perspectives: synergies from co-deployment of negative emission technologies. Biogeosciences 16, 2949–2960. https://doi.org/10.5194/bg-16-2949-2019.

Amann, T., Hartmann, J., Struyf, E., de Oliveira Garcia, W., Fischer, E.K., Janssens, I., Meire, P., Schoelynck, J., 2020. Enhanced weathering and related element fluxes – a cropland mesocosm approach. Biogeosciences 17, 103–119. https://doi.org/10.5194/bg-17-103-2020.

Ameloot, N., Graber, E.R., Verheijen, F.G.A., De Neve, S., 2013. Interactions between biochar stability and soil organisms: review and research needs. Eur. J. Soil Sci. 64, 379–390. https://doi.org/10.1111/ejss.12064.

Amoakwah, E., Shim, J., Kim, S., Lee, Y., Kwon, S., Sangho, J., Park, S., 2023. Impact of silicate and lime application on soil fertility and temporal changes in soil properties and carbon stocks in a temperate ecosystem. Geoderma 433, 116431. https://doi.org/10.1016/j.geoderma.2023.116431.

Anderson, C.R., Condron, L.M., Clough, T.J., Fiers, M., Stewart, A., Hill, R.A., Sherlock, R.R., 2011. Biochar induced soil microbial community change: Implications for biogeochemical cycling of carbon, nitrogen and phosphorus. Pedobiologia 54, 309–320. https://doi.org/10.1016/j.pedobi.2011.07.005.

Azeem, M., Sun, T.-R., Jeyasundar, P.G.S.A., Han, R.-X., Li, H., Abdelrahman, H., Shaheen, S.M., Zhu, Y.-G., Li, G., 2023. Biochar-derived dissolved organic matter (BDOM) and its influence on soil microbial community composition, function, and activity: A review. Crit. Rev. Env Sci. Tec. 1–23. https://doi.org/10.1080/10643389.2023.2190333.

Bakshi, M., Varma, A., 2011. Soil enzyme: the state-of-art. In: Shukla, G., Varma, A. (Eds.), Soil enzymology. Springer Berlin Heidelberg, Berlin, Heidelberg, pp. 1–23.

Bakshi, S., Banik, C., Laird, D.A., 2018. Quantification and characterization of chemically-and thermally-labile and recalcitrant biochar fractions. Chemosphere 194, 247–255. https://doi.org/10.1016/j.chemosphere.2017.11.151.

Bamminger, C., Marschner, B., Jüschke, E., 2014. An incubation study on the stability and biological effects of pyrogenic and hydrothermal biochar in two soils. Eur. J. Soil Sci. 65, 72–82. https://doi.org/10.1111/ejss.12074.

Bates, D., Mächler, M., Bolker, B., Walker, S., 2015. Fitting linear mixed-effects models using lme4. J. Stat. Softw. 67 (1), 48. https://doi.org/10.18637/jss.v067.i01.

Beerling, D.J., Kantzas, E.P., Lomas, M.R., Taylor, L.L., Zhang, S., Kanzaki, Y., Eufrasio, R.M., Renforth, P., Mecure, J.-F., Pollitt, H., Holden, P.B., Edwards, N.R., Koh, L., Epihov, D.Z., Wolf, A., Hansen, J.E., Banwart, S.A., Pidgeon, N.F., Reinhard, C.T., Planavsky, N.J., Val Martin, M., 2025. Transforming US agriculture for carbon removal with enhanced weathering. Nature 638, 425–434. https://doi.org/10.1038/s41586-024-08429-2.

Bekchanova, M., Campion, L., Bruns, S., Kuppens, T., Lehmann, J., Jozefczak, M., Cuypers, A., Malina, R., 2024. Biochar improves the nutrient cycle in sandy-textured soils and increases crop yield: a systematic review. Environ. Evid. 13, 3. https://doi.org/10.1186/s13750-024-00326-5.

Burns, R.G., DeForest, J.L., Marxsen, J., Sinsabaugh, R.L., Stromberger, M.E., Wallenstein, M.D., Weintraub, M.N., Zoppini, A., 2013. Soil enzymes in a changing environment: current knowledge and future directions. Soil Biol. Biochem 58, 216–234. https://doi.org/10.1016/j.soilbio.2012.11.009.

Buss, W., Shepherd, J.G., Heal, K.V., Mašek, O., 2018. Spatial and temporal microscale pH change at the soil-biochar interface. Geoderma 331, 50–52. https://doi.org/10.1016/j.geoderma.2018.06.016.

Buss, W., Yeates, K., Rohling, E., Borevitz, J., 2021. Enhancing natural cycles in agro-ecosystems to boost plant carbon capture and soil storage. Oxf. Open Clim. Change 1. https://doi.org/10.1093/oxfclm/kgab006.

Buss, W., Wurzer, C., Manning, D.A.C., Rohling, E.J., Borevitz, J., Mašek, O., 2022. Mineral-enriched biochar delivers enhanced nutrient recovery and carbon dioxide removal. Commun. Earth Environ. 3, 67. https://doi.org/10.1038/s43247-022-00394-w.

Buss, W., Hasemer, H., Ferguson, S., Borevitz, J., 2023. Stabilisation of soil organic matter with rock dust partially counteracted by plants. bioRxiv. https://doi.org/10.1101/2023.1106.1102.543347, 10.1101/2023.06.02.543347.

Carson, J.K., Rooney, D., Gleeson, D.B., Clipson, N., 2007. Altering the mineral composition of soil causes a shift in microbial community structure. FEMS Microbiol Ecol. 61, 414–423. https://doi.org/10.1111/j.1574-6941.2007.00361.x.

Chagas, J.K.M., Figueiredo, C.Cd, Ramos, M.L.G., 2022. Biochar increases soil carbon pools: evidence from a global meta-analysis. J. Environ. Manag. 305, 114403. https://doi.org/10.1016/j.jenvman.2021.114403.

Chen, M., Liu, D., Shao, X., Li, S., Jin, X., Qi, J., Liu, H., Li, C., Li, C., Li, C., 2024. Effect of biochar types and rates on SOC and its active fractions in tropical farmlands of China. Agronomy 14, 676. https://doi.org/10.3390/agronomy14040676.

Chintala, R., Javier, M., E, S.T., D, M.D., Julson, J.L., 2014. Effect of biochar on chemical properties of acidic soil. Arch. Agron. Soil Sci. 60, 393–404. https://doi.org/10.1080/03650340.2013.789870.

Clough, T., Condron, L.M., Kammann, C., Müller, C., 2013. A review of biochar and soil nitrogen dynamics. Agronomy 3, 275–293. https://doi.org/10.3390/agronomy3020275.

Dai, Z., Zhang, X., Tang, C., Muhammad, N., Wu, J., Brookes, P.C., Xu, J., 2017. Potential role of biochars in decreasing soil acidification - A critical review. Sci. Total Environ. 581-582, 601–611. https://doi.org/10.1016/j.scitotenv.2016.12.169.

Deng, L., Peng, C., Huang, C., Wang, K., Liu, Q., Liu, Y., Hai, X., Shangguan, Z., 2019. Drivers of soil microbial metabolic limitation changes along a vegetation restoration gradient on the Loess Plateau, China. Geoderma 353, 188–200. https://doi.org/10.1016/j.geoderma.2019.06.037.

DIN, 2005. DIN 19746:2005-06: Soil quality - Determination of mineral nitrogen (nitrat and ammonium) in soil profiles (Nmin laboratory method). DIN Media GmbH, Berlin, Germany.

DIN, 2011. EN ISO 14240-2:2011-09: Soil quality - Determination of soil microbial biomass - Part 2: Fumigation-extraction method. DIN Media GmbH, Berlin, Germany, p. 20.

Ding, X., Li, G., Zhao, X., Lin, Q., Wang, X., 2023. Biochar application significantly increases soil organic carbon under conservation tillage: an 11-year field experiment. Biochar 5, 28. https://doi.org/10.1007/s42773-023-00226-w.

Dupla, X., Romane, C., Emma, B., Iris, G., Renée-Claire, L.B., Stéphanie, G., 2024. Let the dust settle: impact of enhanced rock weathering on soil biological, physical, and geochemical fertility. Sci. Total Environ., 176297 https://doi.org/10.1016/j.scitotenv.2024.176297.

Ghodszad, L., Reyhanitabar, A., Maghsoodi, M.R., Asgari Lajayer, B., Chang, S.X., 2021. Biochar affects the fate of phosphorus in soil and water: a critical review. Chemosphere 283, 131176. https://doi.org/10.1016/j.chemosphere.2021.131176.

Glaser, B., Lehr, V.-I., 2019. Biochar effects on phosphorus availability in agricultural soils: a meta-analysis. Sci. Rep. 9, 9338. https://doi.org/10.1038/s41598-019-45693-z.

Glaser, B., Haumaier, L., Guggenberger, G., Zech, W., 2001. The 'Terra Preta' phenomenon: a model for sustainable agriculture in the humid tropics. Naturwissenschaften 88, 37–41. https://doi.org/10.1007/s001140000193.

Gross, A., Bromm, T., Glaser, B., 2021. Soil organic carbon sequestration after biochar application: a global meta-analysis. Agronomy 11, 2474. https://doi.org/10.3390/agronomy11122474.

Guo, F., Sun, H., Yang, J., Zhang, L., Mu, Y., Wang, Y., Wu, F., 2023. Improving food security and farmland carbon sequestration in China through enhanced rock weathering: field evidence and potential assessment in different humid regions. Sci. Total Environ. 903, 166118. https://doi.org/10.1016/j.scitotenv.2023.166118.

Hagemann, N., Spokas, K., Schmidt, H.-P., Kägi, R., Böhler, M.A., Bucheli, T.D., 2018. Activated carbon, biochar and charcoal: linkages and synergies across pyrogenic carbon's ABCs. Water 10, 182. https://doi.org/10.3390/w10020182.

Halmi, M.F.A., Simarani, K., 2021. Responses of soil microbial population and lignocellulolytic enzyme activities to palm kernel shell biochar amendment. Eurasia Soil Sci. 54, 1903–1911. https://doi.org/10.1134/S1064229321120073.

Hamburger, S.E., Meyer zu Drewer, J., Hagemann, N., Geilfus, C.-M., Kammann, C.I., 2026. A crop yield Nitrate leaching dataset A semi-field lysimeter Exp. Cabbage turnip Comb. biochar Rock. powder amend.

Haque, F., Santos, R.M., Chiang, Y.W., 2020. Optimizing inorganic carbon sequestration and crop yield with wollastonite soil amendment in a microplot study. Front Plant Sci. 11. https://doi.org/10.3389/fpls.2020.01012.

Hematimatin, N., Igaz, D., Aydın, E., Horák, J., 2024. Biochar application regulating soil inorganic nitrogen and organic carbon content in cropland in the Central Europe: a seven-year field study. Biochar 6, 14. https://doi.org/10.1007/s42773-024-00307-4.

Hossain, M.Z., Bahar, M.M., Sarkar, B., Donne, S.W., Ok, Y.S., Palansooriya, K.N., Kirkham, M.B., Chowdhury, S., Bolan, N., 2020. Biochar and its importance on nutrient dynamics in soil and plant. Biochar 2, 379–420. https://doi.org/10.1007/s42773-020-00065-z.

Hothorn, T., Bretz, F., Westfall, P., 2008. Simultaneous inference in general parametric models. Biom. J. 50, 346–363. https://doi.org/10.1002/bimj.200810425.

Hu, Y., Abulaizi, M., Tian, Y., Hu, Y., Chen, M., Li, K., Jia, Y., Kou, T., Zhou, J., Jia, H., 2025. Effects of biochar on soil organic carbon stability in degraded alpine grasslands—A study on arid regions in Central Asia. Land 14, 1018. https://doi.org/10.3390/land14051018.

Jin, X., Zhang, T., Hou, Y., Bol, R., Zhang, X., Zhang, M., Yu, N., Meng, J., Zou, H., Wang, J., 2024. Review on the effects of biochar amendment on soil microorganisms and enzyme activity. J. Soil Sediment. https://doi.org/10.1007/s11368-024-03841-7.

Jin, Y., Liang, X., He, M., Liu, Y., Tian, G., Shi, J., 2016. Manure biochar influence upon soil properties, phosphorus distribution and phosphatase activities: a microcosm incubation study. Chemosphere 142, 128–135. https://doi.org/10.1016/j.chemosphere.2015.07.015.

Joergensen, R.G., 1996. The fumigation-extraction method to estimate soil microbial biomass: calibration of the k_{EC} value. Soil Biol. Biochem 28, 25–31. https://doi.org/10.1016/0038-0717(95)00102-6.

Joseph, S.D., Camps-Arbestain, M., Lin, Y., Munroe, P., Chia, C.H., Hook, J., van Zwieten, L., Kimber, S., Cowie, A., Singh, B.P., Lehmann, J., Foidl, N., Smernik, R.J., Amonette, J.E., 2010. An investigation into the reactions of biochar in soil. Soil Res 48, 501–515. https://doi.org/10.1071/SR10009.

Kareem, M.O., Liman, A.H., Odofin, A.J., Azeez, B.A., Musa, B.M., Jimoh, L.T., 2025. Soil organic carbon, cation exchange capacity, and maize (*Zea mays*) response to biochar and nitrogen fertilizer amendments. J. Sci. Res Rep. 31, 278–283. https://doi.org/10.9734/jsrr/2025/v31i53025.

Kassambara, A., 2023. ggcorrplot: Visualization of a correlation matrix using 'ggplot2' - R package version 0.1.4.1.

Komsta, L., 2022. outliers: Tests for outliers - R package version 0.15.

Kuzyakov, Y., Bogomolova, I., Glaser, B., 2014. Biochar stability in soil: decomposition during eight years and transformation as assessed by compound-specific ^{14}C analysis. Soil Biol. Biochem 70, 229–236. https://doi.org/10.1016/j.soilbio.2013.12.021.

Lammirato, C., Miltner, A., Kaestner, M., 2011. Effects of wood char and activated carbon on the hydrolysis of cellobiose by β-glucosidase from *Aspergillus niger*. Soil Biol. Biochem 43, 1936–1942. https://doi.org/10.1016/j.soilbio.2011.05.021.

Le Bas, M.J., Le Maitre, R.W.L., Streckeisen, A., Zanettin, B., Rocks, I.SotSo.I., 1986. A chemical classification of volcanic rocks based on the total alkali-silica diagram. J. Pet. 27, 745–750. https://doi.org/10.1093/petrology/27.3.745.

Lehmann, J., Joseph, S., 2024. Biochar for environmental management: an introduction In. In: Lehmann, J., Joseph, S. (Eds.), Biochar for Environmental Management: Science, Technology and Implementation, 3rd. edition ed. Routledge, London, United Kingdom, p. 14.

Lehmann, J., Rillig, M.C., Thies, J., Masiello, C.A., Hockaday, W.C., Crowley, D., 2011. Biochar effects on soil biota – A review. Soil Biol. Biochem 43, 1812–1836. https://doi.org/10.1016/j.soilbio.2011.04.022.

Lehmann, J., Cowie, A., Masiello, C.A., Kammann, C., Woolf, D., Amonette, J.E., Cayuela, M.L., Camps-Arbestain, M., Whitman, T., 2021. Biochar in climate change mitigation. Nat. Geosci. 14, 883–892. https://doi.org/10.1038/s41561-021-00852-8.

Li, J.-G., Dong, Y.-H., 2013. Effect of a rock dust amendment on disease severity of tomato bacterial wilt. Antonie Van. Leeuwenhoek 103, 11–22. https://doi.org/10.1007/s10482-012-9781-4.

Li, Z.-B., Li, G., Adams, J.M., Guan, D.-X., Zhao, L., Bian, R., Hu, Q., Lu, X., Ji, J., Chen, J., 2025. Atmospheric CO_2 removal efficiency through enhanced silicate weathering in croplands: a review with emphasis on the contribution of fungi. J. Earth Sci. 36, 197–211. https://doi.org/10.1007/s12583-024-0101-5.

Liang, B., Lehmann, J., Solomon, D., Kinyangi, J., Grossman, J., O'Neill, B., Skjemstad, J.O., Thies, J., Luizão, F.J., Petersen, J., Neves, E.G., 2006. Black carbon increases cation exchange capacity in soils. Soil Sci. Soc. Am. J. 70, 1719–1730. https://doi.org/10.2136/sssaj2005.0383.

Liao, X., Kang, H., Haidar, G., Wang, W., Malghani, S., 2022. The impact of biochar on the activities of soil nutrients acquisition enzymes is potentially controlled by the pyrolysis temperature: a meta-analysis. Geoderma 411, 115692. https://doi.org/10.1016/j.geoderma.2021.115692.

Liu, S., Zhang, Y., Zong, Y., Hu, Z., Wu, S., Zhou, J., Jin, Y., Zou, J., 2015. Response of soil carbon dioxide fluxes, soil organic carbon and microbial biomass carbon to biochar amendment: a meta-analysis. GCB Bioenergy 8, 392–406. https://doi.org/10.1111/gcbb.12265.

Loeppmann, S., Blagodatskaya, E., Pausch, J., Kuzyakov, Y., 2016. Enzyme properties down the soil profile - A matter of substrate quality in rhizosphere and detritusphere. Soil Biol. Biochem 103, 274–283. https://doi.org/10.1016/j.soilbio.2016.08.023.

Luo, L., Meng, H., Gu, J.-D., 2017. Microbial extracellular enzymes in biogeochemical cycling of ecosystems. J. Environ. Manag. 197, 539–549. https://doi.org/10.1016/j.jenvman.2017.04.023.

Marx, M.C., Wood, M., Jarvis, S.C., 2001. A microplate fluorimetric assay for the study of enzyme diversity in soils. Soil Biol. Biochem 33, 1633–1640. https://doi.org/10.1016/S0038-0717(01)00079-7.

Medeiros, F.P., Theodoro, S.H., Carvalho, A.M.X., Oliveira, V.S., Oliveira, L.C., Almeida, R.M.P., Viana, M.B., Gomide, C.S., 2025. The combination of crushed rock and organic matter enhances the capture of inorganic carbon in tropical soils. J. S Am. Earth Sci. 152, 105254. https://doi.org/10.1016/j.jsames.2024.105254.

Meyer zu Drewer, J., Vorrath, M.-E., Amann, T., Hartmann, J., De la Rosa, J.M., Möllmer, J., Pérez-Dalí, S.M., Meredith, W., Uguna, C., Snape, C., Kammann, C., Schmidt, H.-P., Hagemann, N., 2025. Pyrogenic carbon and carbonating minerals for carbon capture and storage (PyMiCCS) part I: production, physico-chemical characterization and C-sink potential. Front Clim. 7, 2025. https://doi.org/10.3389/fclim.2025.1631368.

Michaelis, L., Menten, M.L., 1913. Die kinetik der invertinwirkung. Biochem. Z. 333–369.

Moorhead, D.L., Sinsabaugh, R.L., Hill, B.H., Weintraub, M.N., 2016. Vector analysis of ecoenzyme activities reveal constraints on coupled C, N and P dynamics. Soil Biol. Biochem 93, 1–7. https://doi.org/10.1016/j.soilbio.2015.10.019.

Ndossi, E.M., Becker, J.N., Hemp, A., Dippold, M.A., Kuzyakov, Y., Razavi, B.S., 2020. Effects of land use and elevation on the functional characteristics of soil enzymes at Mt. Kilimanjaro. Eur. J. Soil Biol. 97, 103167. https://doi.org/10.1016/j.ejsobi.2020.103167.

Qiu, H., Hu, Z., Liu, J., Zhang, H., Shen, W., 2023. Effect of biochar on labile organic carbon fractions and soil carbon pool management index. Agronomy 13, 1385. https://doi.org/10.3390/agronomy13051385.

Rechberger, M.V., Kloss, S., Rennhofer, H., Tintner, J., Watzinger, A., Soja, G., Lichtenegger, H., Zehetner, F., 2017. Changes in biochar physical and chemical properties: accelerated biochar aging in an acidic soil. Carbon 115, 209–219. https://doi.org/10.1016/j.carbon.2016.12.096.

Reginato, P.L., 2025. Biotechnology in direct air capture, enhanced weathering, and methane removal: emerging opportunities and gaps. Front Clim. 6. https://doi.org/10.3389/fclim.2024.1440833.

Reis, B.R., Vasconcelos, A.L.S., Silva, A.M.M., Andreote, F.D., Azevedo, A.C., 2024. Changes in soil bacterial community structure in a short-term trial with different silicate rock powders. Chem. Biol. Technol. Agric. 11, 61. https://doi.org/10.1186/s40538-024-00586-w.

Schmidt, H.-P., Kammann, C., Hagemann, N., Leifeld, J., Bucheli, T.D., Sánchez Monedero, M.A., Cayuela, M.L., 2021. Biochar in agriculture – A systematic review of 26 global meta-analyses. GCB Bioenergy 13, 1708–1730. https://doi.org/10.1111/gcbb.12889.

Shepherd, J.G., Joseph, S., Sohi, S.P., Heal, K.V., 2017. Biochar and enhanced phosphate capture: mapping mechanisms to functional properties. Chemosphere 179, 57–74. https://doi.org/10.1016/j.chemosphere.2017.02.123.

Shi, W., 2011. Agricultural and ecological significance of soil enzymes: soil carbon sequestration and nutrient cycling. In: Shukla, G., Varma, A. (Eds.), Soil enzymology. Springer Berlin Heidelberg, Berlin, Heidelberg, pp. 43–60.

Sinsabaugh, R.L., Lauber, C.L., Weintraub, M.N., Ahmed, B., Allison, S.D., Crenshaw, C., Contosta, A.R., Cusack, D., Frey, S., Gallo, M.E., Gartner, T.B., Hobbie, S.E., Holland, K., Keeler, B.L., Powers, J.S., Stursova, M., Takacs-Vesbach, C., Waldrop, M.P., Wallenstein, M.D., Zak, D.R., Zeglin, L.H., 2008. Stoichiometry of soil enzyme activity at global scale. Ecol. Lett. 11, 1252–1264. https://doi.org/10.1111/j.1461-0248.2008.01245.x.

Sokol, N.W., Sohng, J., Moreland, K., Slessarev, E., Goertzen, H., Schmidt, R., Samaddar, S., Holzer, I., Almaraz, M., Geoghegan, E., Houlton, B., Montañez, I., Pett-Ridge, J., Scow, K., 2024. Reduced accrual of mineral-associated organic matter after two years of enhanced rock weathering in cropland soils, though no net losses of soil organic carbon. Biogeochemistry. https://doi.org/10.1007/s10533-024-01160-0.

Steiner, C., Teixeira, W.G., Lehmann, J., Nehls, T., de Macêdo, J.L.V., Blum, W.E.H., Zech, W., 2007. Long term effects of manure, charcoal and mineral fertilization on crop production and fertility on a highly weathered Central Amazonian upland soil. Plant Soil 291, 275–290. https://doi.org/10.1007/s11104-007-9193-9.

Streckeisen, A., 1980. Classification and nomenclature of volcanic rocks, lamprophyres, carbonatites and melilitic rocks IUGS Subcommission on the Systematics of Igneous Rocks. Geol. Rundsch. 69, 194–207. https://doi.org/10.1007/BF01869032.

Swoboda, P., Döring, T.F., Hamer, M., 2022. Remineralizing soils? The agricultural usage of silicate rock powders: a review. Sci. Total Environ. 807, 150976. https://doi.org/10.1016/j.scitotenv.2021.150976.

Van Zwieten, L., Kimber, S., Morris, S., Chan, K.Y., Downie, A., Rust, J., Joseph, S., Cowie, A., 2010. Effects of biochar from slow pyrolysis of papermill waste on agronomic performance and soil fertility. Plant Soil 327, 235–246. https://doi.org/10.1007/s11104-009-0050-x.

Vance, E.D., Brookes, P.C., Jenkinson, D.S., 1987. An extraction method for measuring soil microbial biomass C. Soil Biol. Biochem 19, 703–707. https://doi.org/10.1016/0038-0717(87)90052-6.

VDLUFA, 1991. Bestimmung von phosphor und kalium im doppellactat(DL)-auszug, methodenbuch band I böden. Verband Deutscher Landwirtschaftlicher Untersuchungs- und Forschungsanstalten e.V. VDLUFA, Speyer, Germany.

Vicca, S., Goll, D.S., Hagens, M., Hartmann, J., Janssens, I.A., Neubeck, A., Peñuelas, J., Poblador, S., Rijnders, J., Sardans, J., Struyf, E., Swoboda, P., van Groenigen, J.W., Vienne, A., Verbruggen, E., 2022. Is the climate change mitigation effect of enhanced silicate weathering governed by biological processes? Glob. Chang Biol. 28, 711–726. https://doi.org/10.1111/gcb.15993.

von Mersi, W., Kuhnert-Finkernagel, R., Schinner, F., 1992. The influence of rock powders on microbial activity of three forest soils. Z. Pflanz. Bodenkd. 155, 29–33. https://doi.org/10.1002/jpln.19921550107.

Vorrath, M.-E., Amann, T., Meyer zu Drewer, J., Hagemann, N., Aldrich, C., Börker, J., Seedtke, M., Becker, J.N., Hagens, M., Eschenbach, A., Hartmann, J., 2025. Pyrogenic carbon and carbonating minerals for carbon capture and storage (PyMiCCS) part II: organic and inorganic carbon dioxide removal in an Oxisol. Front Clim. 7, 2025. https://doi.org/10.3389/fclim.2025.1592454.

Wang, J., Xiong, Z., Kuzyakov, Y., 2016. Biochar stability in soil: meta-analysis of decomposition and priming effects. GCB Bioenergy 8, 512–523. https://doi.org/10.1111/gcbb.12266.

Wang, J., Sun, L., Sun, Y., Yang, S., Qin, Q., Xue, Y., 2025a. Long-term biochar-based fertilizer substitution promotes carbon, nitrogen, and phosphorus acquisition enzymes in dryland soils by affecting soil properties and regulating bacterial community. Appl. Soil Ecol. 206, 105801. https://doi.org/10.1016/j.apsoil.2024.105801.

Wang, X., Li, G., Ali, A., Algora, C., Delgado-Baquerizo, M., Goll, D.S., Vicca, S., Xu, T., Bi, B., Chen, Q., Lin, L., Fang, Y., Hao, Z., Li, Z., Yuan, Z., 2025b. Enhanced rock weathering boosts ecosystem multifunctionality via improving microbial networks complexity in a tropical forest plantation. J. Environ. Manag. 373, 123477. https://doi.org/10.1016/j.jenvman.2024.123477.

Werth, M., Kuzyakov, Y., 2010. ^{13}C fractionation at the root–microorganisms–soil interface: a review and outlook for partitioning studies. Soil Biol. Biochem 42, 1372–1384. https://doi.org/10.1016/j.soilbio.2010.04.009.

Wickham, H., 2016. ggplot2: Elegant graphics for data analysis, 2nd edition ed. Springer, New York, USA.

Wiedner, K., Schneeweiß, J., Dippold, M.A., Glaser, B., 2015. Anthropogenic dark earth in Northern Germany — the nordic analogue to *terra preta de Índio* in Amazonia. CATENA 132, 114–125. https://doi.org/10.1016/j.catena.2014.10.024.

Xiao, L., Min, X., Li, Z., Li, P., 2024. Kinetic and thermodynamic characteristics of soil enzymes in pure and mixed forest samples on the Loess Plateau of China. J. Plant Nutr. Soil Sci. N./a. https://doi.org/10.1002/jpln.202400242.

Xu, Q., Zhang, F., Song, F., Guo, H., Wang, X., Bi, F., Xu, M., 2024a. Investigating CO_2 sequestration via enhanced rock weathering: effects of temperature and citric acid on dolomite and basalt. J. Clean. Prod. 485, 144414. https://doi.org/10.1016/j.jclepro.2024.144414.

Xu, T., Yuan, Z., Vicca, S., Goll, D.S., Li, G., Lin, L., Chen, H., Bi, B., Chen, Q., Li, C., Wang, X., Wang, C., Hao, Z., Fang, Y., Beerling, D.J., 2024b. Enhanced silicate weathering accelerates forest carbon sequestration by stimulating the soil mineral carbon pump. Glob. Chang Biol. 30, e17464. https://doi.org/10.1111/gcb.17464.

Yang, F., Wang, W., Wu, Z., Peng, J., Xu, H., Ge, M., Lin, S., Zeng, Y., Sardans, J., Wang, C., Peñuelas, J., 2024. Fertilizer reduction and biochar amendment promote soil mineral-associated organic carbon, bacterial activity, and enzyme activity in a jasmine garden in southeast China. Sci. Total Environ., 176300 https://doi.org/10.1016/j.scitotenv.2024.176300.

Yang, Y., Liang, C., Wang, Y., Cheng, H., An, S., Chang, S.X., 2020. Soil extracellular enzyme stoichiometry reflects the shift from P- to N-limitation of microorganisms with grassland restoration. Soil Biol. Biochem 149, 107928. https://doi.org/10.1016/j.soilbio.2020.107928.

Zhao, S., Ta, N., Li, Z., Yang, Y., Zhang, X., Liu, D., Zhang, A., Wang, X., 2018. Varying pyrolysis temperature impacts application effects of biochar on soil labile organic carbon and humic fractions. Appl. Soil Ecol. 123, 484–493. https://doi.org/10.1016/j.apsoil.2017.09.007.

Zhou, X., Shen, Y., Fu, X., Wu, F., 2018. Application of sodium silicate enhances cucumber resistance to fusarium wilt and alters soil microbial communities. Front Plant Sci. 9. https://doi.org/10.3389/fpls.2018.00624.

Zimmerman, A.R., 2010. Abiotic and microbial oxidation of laboratory-produced black carbon (biochar). Environ. Sci. Technol. 44, 1295–1301. https://doi.org/10.1021/es903140c.

Glossary

Abbreviation: Definition
AMC: 7-amido-4-methylcoumarin
AP: Acid phosphatase (P-acquiring enzyme)
BC: Biochar treatment
BG: ß-glucosidase (C-acquiring enzyme)
C: Carbon (element) or in this case total carbon content of the soil
CDR: Carbon dioxide removal
CEC: Cation exchange capacity
CFE: Chloroform fumigation extraction (to determine C_{mic})
CH: Chitinase (C- and N-acquiring enzyme)
C_{mic}: Microbial biomass carbon
Co-app.: Co-application treatment containing biochar and basanite
Co-pyr.: Co-pyrolysis treatment containing rock-enhanced biochar
DOC: Dissolved organic carbon
EC: Electric conductivity
EES: Extracellular enzyme stoichiometry
ERW: Enhanced rock weathering
K_a: Catalytic enzyme efficiency
K_m: Enzyme binding affinity
LAP: Leucine-aminopeptidase (N-acquiring enzyme)
LME: Linear mixed effect model

MUF: 4-methylumbelliferon
N: Nitrogen (element) or in this case total nitrogen content of the soil
N_{min}: Mineral nitrogen
P: Phosphorous (element)
RP: Rock powder treatment containing basanite
TIC: Total inorganic carbon
TOC: Total organic carbon
v: Reaction rate of an enzyme
V_{max}: Potential maximum enzyme activity
WC: Water content